University of Central Lancashire
UCLan

Central Lancashire Online Knowledge (CLoK)

Title	Human Helicase RECQL4 Drives Cisplatin Resistance in Gastric Cancer by Activating an AKT-YB1-MDR1 Signaling Pathway
Type	Article
URL	https://clok.uclan.ac.uk/id/eprint/34532/
DOI	https://doi.org/10.1158/0008-5472.CAN-15-2361
Date	2016
Citation	Mo, Dongliang, Fang, Hongbo, Niu, Kaifeng, Liu, Jing, Wu, Meng, Li, Shiyou, Zhu, Tienian, Aleskandarany, Mohammed, Arora, Arvind et al (2016) Human Helicase RECQL4 Drives Cisplatin Resistance in Gastric Cancer by Activating an AKT-YB1-MDR1 Signaling Pathway. Cancer Research, 76 (10). pp. 3057-3066. ISSN 0008-5472
Creators	Mo, Dongliang, Fang, Hongbo, Niu, Kaifeng, Liu, Jing, Wu, Meng, Li, Shiyou, Zhu, Tienian, Aleskandarany, Mohammed, Arora, Arvind, Lobo, Dileep N., Madhusudan, Srinivasan, Balajee, Adayabalam S., Chi, Zhenfen and Zhao, Yongliang

It is advisable to refer to the publisher's version if you intend to cite from the work.
https://doi.org/10.1158/0008-5472.CAN-15-2361

For information about Research at UCLan please go to http://www.uclan.ac.uk/research/

All outputs in CLoK are protected by Intellectual Property Rights law, including Copyright law. Copyright, IPR and Moral Rights for the works on this site are retained by the individual authors and/or other copyright owners. Terms and conditions for use of this material are defined in the http://clok.uclan.ac.uk/policies/

Human helicase RECQL4 drives cisplatin resistance in gastric cancer by activating an AKT-YB1-MDR1 signaling pathway

Dongliang Mo[1,2], Hongbo Fang[1], Kaifeng Niu[1,2], Jing Liu[1,2,3], Meng Wu[4], Shiyou Li[1], Tienian Zhu[5], Mohammed A. Aleskandarany[6], Arvind Arora[6], Dileep N. Lobo[7], Srinivasan Madhusudan[6], Adayabalam S. Balajee [8], Zhenfen Chi[1,*], Yongliang Zhao[1,*]

[1]Key Laboratory of Genomic and Precision Medicine, China Gastrointestinal Cancer Research Center, Beijing Institute of Genomics, Chinese Academy of Sciences, Beijing 100101, China

[2]University of Chinese Academy of Sciences, Beijing 100049, China

[3]Current address: Dalian Institute of Chemical Physics, Chinese Academy of Sciences, 457 Zhongshan Road, Dalian 116023, China

[4]Biological Institute, Hebei Academy of Sciences, Shijiazhuang 050081, China

[5]Department of Medical Oncology, Bethune International Peace Hospital, Shijiazhuang 050082, China

[6]Division of Cancer and Stem Cells, School of Medicine, University of Nottingham, Nottingham University Hospitals, City Hospital Campus, Nottingham NG51PB, UK.

[7]Gastrointestinal Surgery, National Institute for Health Research Nottingham Digestive Diseases Centre Biomedical Research Unit, Nottingham University Hospitals and University of Nottingham, Queen's Medical Centre, Nottingham NG7 2UH, UK.

[8]REAC/TS, Oak Ridge Associated Universities, Oak Ridge Institute for Science and Education, 1299 Bethel Valley Road, Oak Ridge, TN37830

D. Mo and H. Fang contributed equally to the work

***Corresponding authors:**

Yongliang Zhao, Phone：8610-84097648, Fax: 8610-84097648, Email: zhaoyongliang@big.ac.cn and Zhenfen Chi, Phone: 8610-84097746, Fax: 8610-84097720, Email: chizf@big.ac.cn.

Running Title: RECQL4 modulates MDR1 expression and chemo resistance

Disclosure of potential conflicts of interest

No potential conflicts of interest were disclosed

Financial support

This work was supported by the National Basic Research Program of China (973 program; No. 2013CB91100 and 2015CB910600), the National Natural Science Foundation of China (No. 81272929, 31570815), CAS Key Research program (No. KJZD-EW-L14).

Abstract

Elevation of the DNA unwinding helicase RECQL4 which participates in various DNA repair pathways has been suggested to contribute to the pathogenicity of various human cancers, including gastric cancer. In this study, we addressed the prognostic and chemotherapeutic significance of RECQL4 in human gastric cancer (GC) which has yet to be determined. We observed significant increases in RECQL4 mRNA or protein in >70% of three independent sets of human GC specimens examined, relative to normal gastric tissues. Strikingly, high RECQL4 expression in primary tumors correlated well with poor survival and GC lines with high RECQL4 expression displayed increased resistance to cisplatin treatment. Mechanistic investigations revealed a novel role for RECQL4 in transcriptional regulation of the multidrug resistance gene MDR1, through a physical interaction with the transcription factor YB1. Notably, ectopic expression of RECQL4 in cisplatin-sensitive GC cells with low endogenous RECQL4 was sufficient to render them resistant to cisplatin, in a manner associated with YB1 elevation and MDR1 activation. Conversely, RECQL4 silencing in cisplatin-resistant GC cells with high endogenous RECQL4 suppressed YB1 phosphorylation, reduced MDR1 expression and re-sensitizes cells to cisplatin. In establishing RECQL4 as a critical mediator of cisplatin resistance in GC cells, our findings provide a therapeutic rationale to target RECQL4 or the downstream AKT-YB1-MDR1 axis to improve GC treatment.

Key words: RECQL4 elevation, YB1, MDR1 activation, cisplatin resistance.

Introduction

Systemic chemotherapy is the main treatment option for gastric cancer (GC) patients as GC is often diagnosed at an advanced stage and surgical removal is not feasible. However, prognosis and clinical response are highly variable even for the same grade and stage of the tumors and chemo resistance chiefly contributes to treatment failure and recurrence in GC patients (1). Therefore, understanding the molecular/mechanistic basis for the chemo resistance in GC is essential not only for devising a better treatment modality but also for developing new chemo sensitization strategies to improve GC patient survival in the future.

Cisplatin (cis-diamminedichloroplatinum) is one of the most frequently used chemotherapeutic drugs in clinical GC treatment settings. The most prominent mode of its action is to initiate an intrinsic apoptotic pathway through DNA damage response activation (2). Many GC patients display cisplatin resistance through multiple mechanism(s) including a decreased uptake and/or an increased efflux of cisplatin mediated by specific transporters, such as *MDRs* and *ATP7B* (3-5). Also, constitutive activation of DNA damage response (DDR) pathways owing to elevated expression of DNA repair genes also contributes to chemo resistance by efficient reversal of cisplatin-DNA adducts (6).

RECQL4, a member of RECQ helicase family with DNA-unwinding activity (7), plays an important role in maintaining the stability of nuclear (8) and mitochondrial

genomes (9-11). This is well supported by the existence of three human autosomal recessive disorders Rothmund-Thomson syndrome (RTS) (12), RAPADILLINO (13) and Baller-Gerold syndrome (BGS), all of them owing to mutations in RECQL4 (14). Mutational loss of *RECQL4* is associated with increased risk for osteosarcoma development in RTS patients (15). Additionally, primary fibroblasts from RTS patients have an increased sensitivity to genotoxic agents (16). *RECQL4* had recently been found to be significantly associated with clinical outcome and *RECQL4* suppression sensitized the breast cancer cells to DNA damaging agents (17, 18).

Although aberrant expression of *RECQL4* has been reported in sporadic osteoblastoma (19), breast and prostate cancer cells and tissues (20, 21), its prognostic and chemotherapeutic significance in GC are not known. In this study, we demonstrated *RECQL4* expression is aberrantly elevated frequently in both clinical GC samples and tumor cell lines, and a higher *RECQL4* expression renders the GC cells more resistance to cisplatin treatment. We further established a molecular link between *RECQL4* expression and cisplatin resistance, in which RECQL4 potentiates YB1 phosphorylation through enhancing AKT and YB1 interaction, suggesting that *RECQL4* is a critical determinant of cisplatin resistance in GC cells through regulation of AKT-YB1-MDR1 pathway.

Materials and Methods

Cell lines and antibodies

The human embryonic kidney HEK293 cell line was ordered in 2012, gastric

cancer cell lines AGS and NCI-N87 were ordered in 2013, and SNU-1 and SNU-16 were ordered in 2015 from ATCC. MKN45 and HGC-27 were ordered in 2013 from the Japanese Collection of Research Bioresources and the European Collection of Cell Culture, UK, respectively. MGC-803 was ordered in 2013 from Cell Resource Center, Chinese Academy of Medical Sciences, and authenticated using Short Tandem Repeat (STR) profiling analysis by this Center on Dec. 30, 2015. MKN45, SNU-1 and SNU-16 cell lines were STR-authenticated on Nov. 24, 2015 by Cobioer Biosciences Co. LTD, Nanjing, China. AGS, NCI-N87, HGC-27 and HEK293 were STR-authenticated on Dec. 8, 2015 by Shanghai Biowing Applied Biotechnology Co. LTD, Shanghai, China.

Antibodies: RECQL4 from Novus Biologicals (#25470002) and Cell signaling (#2814); AKT (#9272), p-AKT (#9271), YB1 (#4202) and p-YB1 (#2900) from Cell Signaling; MVP (ab175239) and MDR1 (ab129450) from Abcam; GAPDH (MAB374) from Millipore and β-actin (A1978) from Sigma.

GC tissue array and clinical samples

TissueScan Human gastroesophogeal cancer tissue qPCR array was ordered from Origene (#HGRT101, Rockville, MD 20850). Eleven pairs of human gastric adenocarcinomas and matched normal gastric specimens were collected from the Department of Medical Oncology, Bethune International Peace Hospital, Shijiazhuang, China. The study on human GC samples has been approved by the Ethics Committee of Beijing Institute of Genomics.

Immunohistochemistry (IHC) on GC patient samples

Patient demographics about 142 gastric adenocarcinoma cases treated at Nottingham University Hospitals (NUH) between 2001 and 2006 were summarized in Supplementary Table S1. This cohort, comprised of well-characterized patient samples, was used for a wide range of biomarker studies (22-24). Approval from the Ethics Committee of Nottingham University Hospital, UK was obtained for this study.

RECQL4 expression was carried out on TMA slides with the primary anti-RECQL4 antibody (#25470002, Novus Biologicals) at a dilution of 1:175. Whole field inspection of the core was scored and intensities of nuclear or cytoplasmic staining were grouped as follows: 0 = no staining, 1 = weak staining, 2 = moderate staining, 3 = strong staining. The percentage of each category was estimated (0-100%). H-score (range 0-300) was calculated by multiplying intensity of staining and percentage staining. Low/negative RECQL4 cytoplasmic expression was defined by mean of H-score of <122. Low/negative RECQL4 nuclear expression was defined by mean of H-score of <179.

Statistical analysis

Statistical analysis of data was performed using SPSS version 20.0 for Windows (SPSS Inc, Chicago, IL, USA). Survival rates were calculated from the time of diagnosis until the end of the follow up period and Kaplan Meier curves were plotted.

The statistical significance of differences between survival rates was determined using the log-rank test. P values ≤ 0.05 was considered as statistically significant.

MTT assay and cisplatin treatment

Cell survival was measured by the 3-(4,5-dimethylthiazol-2-yl)-2,5-diphenyltetrazolium bromide (MTT) assay. Cells were seeded at a density of 5,000 cells per well in 96-well plates and incubated at 37℃ in humidified 5% CO_2 for 12 h. Cells were then exposed to different concentrations of cisplatin for 72 h, and cellular viability was quantified by the MTT assay following the manufacturer's instructions (Molecular Probes). Absorbance values at 540 nm were read on a Spectra Max 250 spectrophotometer (Molecular Devices). All MTT assays include 10 duplicated wells for each time-point of each cell line. The data represent mean ± SD from three independent experiments.

Dual-Luciferase assay

A 256 bp length of MDR1 gene promoter region (−188-+68) containing Y-box consensus sequence used for luciferase reporter assay was amplified by PCR using the following primer pair: forward: 5'-ggggtaccGCAACGGAAGCCAGAACATT-3', reverse: 5'-cccaagcttTGGAAAGACCTAAAGGAAACGA-3'. The PCR fragment was then cloned into the KpnI/HindIII sites of pGL3-Basic vector, and verified by sequencing. The pGL3-MDR1pro plasmid was transiently transfected into YB1-silenced MGC803/Tet-on/Flag-RECQL4 cells with YB1 reconstitution or/and

Dox-induced expression of RECQL4. Luciferase activity was measured following the dual-luciferase assay protocol (Promega).

Adenovirus vector-mediated knock down of *RECQL4* and *YB1* expression

To generate *shRECQL4* and *shYB1* Adenovirus constructs, a 21 mer *RECQL4* shRNA (GCTCAAGGCCAATCTGAAAGG, 366–386, Accession No. NM_004260) and two 21 mer *YB1* shRNAs (GGTCATCGCAACGAAGGTT, 330-348; GGTTCCCACCTTACTACAT, 746-764, Accession No. NM_004559.3) were cloned into U6 promoter pshuttle vector (Agilent), respectively. The scrambled 21 mer control shRNA sequence is GAAGAGGACACGCCTTAGACT. Adenovirus particles were produced in HEK293 packaging cells, and used for infecting the cells using the AdEasy Adenoviral Vector System following the manufacture's protocol (Cell Biolabs, Inc, USA). Two *YB1* shRNA adenovirus were used concurrently for knocking down *YB1* expression.

Results

***RECQL4* expression is up regulated in human gastric cancer samples**

To verify whether or not *RECQL4* expression is aberrantly elevated in human GC cells, *RECQL4* mRNA level was first determined by real-time quantitative PCR using TissueScan Human gastroesophageal cancer tissue qPCR array (Origene). This array contains cDNA samples of 3 normal gastric tissues (*marked), and 20 GC samples (*marked) with different pathological grades. Other specimens include 3

normal esophageal and 20 esophageal tumor tissues (unmarked). As shown in Figure 1A, 75% (15/20) of GC tissues displayed a 2.5-fold higher level of *RECQL4* mRNA than normal tissues. RECQL4 protein level was next examined by Western blotting in 11 pairs of human GC samples and matched normal controls. In corroboration with elevated *RECQL4* mRNA expression in the clinical GC samples, RECQL4 protein elevation was also observed in 8/11 GC samples (Fig. 1B).

High cytoplasmic *RECQL4* expression correlates with poor survival of GC patients

In this study, 92 of 148 tumor cores were found suitable for analysis as some cores within the TMA were missing or lacked tumor and these were eliminated from analysis. Low levels of nuclear and cytoplasmic RECQL4 expression were found in 18 of 92 (19.6%) samples, while 29 of 92 (31.5%) samples showed high nuclear and low cytoplasmic expression. Further, low nuclear/high cytoplasmic RECQL4 expression was observed in 22 of 92 (23.9%) samples and high nuclear/high cytoplasmic RECQL4 was found in 23 of 92 (25%) samples (Figure 1C). As shown in Supplementary Table S2, compared to tumors with low RECQL4 protein expression, RECQL4 high nuclear or high nuclear/cytoplasmic co-expression correlated well with grade III tumors ($p=0.048$), tumor vascular invasion ($p=0.001$) and circumferential resection margin ($p=0.041$), suggesting that RECQL4 high expression has a potential role during GC tumor progression. Interestingly, tumors with high cytoplasmic RECQL4 expression had poor disease specific survival

(p=0.05). While RECQL4 nuclear expression alone did not influence survival (p=0.547), tumors with both high nuclear/cytoplasmic RECQL4 appeared to have poor survival compared to tumors with low nuclear/cytoplasmic RECQL4 expression (p=0.05, Fig.1D). It is to be mentioned that these patients received only surgery but not any adjuvant/neoadjuvant chemotherapy.

RECQL4 gene is wild type in both GC cells and clinical GC specimens with high _RECQL4_ expression

To clarify whether or not the oncogenic property is driven by gain of function owing to mutations in *RECQL4*, the status of *RECQL4* gene was analyzed in 7 GC cell lines and 11 human surgical GC specimens by PCR-based single-strand conformation polymorphism (PCR-SSCP) analysis. The primer sets for 21 exons of *RECQL4* coding region and sizes of PCR products were summarized in Supplementary Table S3. As shown in Supplementary Fig. S1-3, abnormal SSCP band migration in comparison with normal control was observed only in exons 2-3 of *RECQL4* gene in AGS and HGC-27 tumor cells. Further sequencing results demonstrated a synonymous GAG to GAA mutation (Glu-Glu at aa 44) in both cell types. In support, genetic polymorphism at this locus has been reported previously by others (12, 25). These results clearly demonstrated that *RECQL4* is wild-type in both GC cells and surgical GC specimens.

Elevated _RECQL4_ expression renders the GC cells more resistant to cisplatin

treatment

We wished to verify whether or not elevated *RECQL4* expression confers cisplatin resistance in GC cells. For this purpose, we first examined the RECQL4 protein level in 7 GC cell lines in relative to normal gastric epithelium. In corroboration with elevated *RECQL4* mRNA expression in the clinical GC samples, RECQL4 protein level was also elevated in all the GC cell lines with a much higher level in 4 of the 7 cell lines including AGS, NCI-N87, HGC-27 and SNU-16 when compared to normal control (Fig. 2A). Then the sensitivity to cisplatin treatment was tested by seeding the GC cells at a density of 5,000 cells and treated with graded concentrations of cisplatin (0, 0.5, 1, 1.5, 2, 2.5 μg/ml). Cell viability was quantified by the MTT assay. As shown in Figure 2B, NCI-N87, AGS and SNU-16 cells with high *RECQL4* expression displayed a significantly higher resistance to cisplatin treatment. In contrast, a much lower cisplatin resistance was observed in MGC-803 cells with a relatively lower *RECQL4* expression. Three cell lines with high (HGC-27) and low (MKN45, SNU-1) *RECQL4* expression showed an intermediate response to cisplatin. Taken together, our results showed a reasonably good correlation between *RECQL4* expression and cisplatin resistance for most of the GC cell lines examined.

RECQL4 physically interacts with YB1

Correlation observed between *RECQL4* expression and cisplatin resistance prompted us to examine the downstream signaling pathway(s) that may be regulated by *RECQL4*. Immunoprecipitation coupled with mass spectrometry was performed

using the lysates of *Flag-RECQL4* transfected HEK293 cells. Among the list of candidates identified to interact with RECQL4, YB1 was chosen because YB1 had the highest score in mass spectrometry analysis. Furthermore, YB1 was demonstrated to be not only a transcription factor but also involved in multidrug resistance through regulation of downstream genes such as *MDR1* and major vault protein (*MVP*) *genes* (26, 27). Interaction between RECQL4 and YB1 was then tested in Flag-RECQL4 overexpressed U2OS cells by co-IP assay. Endogenous YB1 was detected in anti-Flag pull-down lysate with anti-YB1 antibody by Western blotting (Fig. 3A). Likewise, endogenous RECQL4 was observed in anti-YB1 pull-down complex (Fig. 3B), illustrating the interaction between RECQL4 and YB1. YB1 has been shown to be downstream substrate for AKT (28). In support, AKT was detected in the immunoprecipitated complex using either anti-Flag to Flag-RECQL4 or anti-YB1 antibodies (Fig. 3A & 3B), suggesting that RECQL4 physically interacts with YB1 and AKT.

To further confirm the nature of interaction, purified GST-AKT, His-YB1 and His-RECQL4-Flag proteins expressed in *E. coli* BL21 and detected by Coomassie brilliant blue staining (Supplementary Fig. S4) were used for the *in vitro* pull-down assays. Purified His-RECQL4-Flag protein was immobilized on Flag beads and then incubated with His-YB1. Purified GST-AKT was immobilized on glutathione Sepharose beads, and incubated with His-YB1 and/or His-RECQL4-Flag protein. Consistent with the IP results, His-YB1 was pulled down with His-RECQL4-Flag (Fig. 3C), and also with GST-AKT not by GST alone (Fig. 3D), suggesting a direct

interaction between RECQL4 and YB1 as well as AKT and YB1. His-RECQL4-Flag can only be pulled down by GST-AKT in the presence of YB1 (Fig. 3D), suggesting an YB1-dependent interaction between RECQL4 and AKT. Through mapping the domain of YB1 protein specifically interacting with RECQL4 using various GFP-YB1 mutants, the fragment 130-205 aa of YB1 was demonstrated to be responsible for the interaction with RECQL4 (Supplementary Fig. S5).

AKT and YB1 association was enhanced in the presence of RECQL4

Observation of physical interaction between RECQL4 and YB1 prompted us to examine whether or not RECQL4 promotes the association of YB1 with AKT. *In vitro* pull-down assay (Fig. 3E) revealed that AKT and YB1 interaction was markedly increased by 2.3- to 5.7-fold when RECQL4 protein input was increased from 0 to 0.2 μg (+) and 1 μg (++), respectively. Additionally, YB1 and AKT interaction was detected mainly in the cytoplasmic fraction, and their interaction in the cytoplasmic fraction was substantially enhanced when RECQL4 was induced in MGC-803/Tet-on/Flag-RECQL4 cells (Supplementary Fig. S6).

RECQL4 promotes AKT-dependent YB1 phosphorylation

It has been reported previously that YB1, being one of the substrates for AKT, enters into nuclear compartment and binds to the promoter region of targeted genes when phosphorylated by AKT (29). Our findings of enhanced association of YB1 and AKT by RECQL4 led us to investigate whether or not *RECQL4* regulates the level of

YB1 phosphorylation in GC cells. AGS cells with high *RECQL4* expression and RECQL4-inducible MGC-803 cells with low RECQL4 expression were used for evaluating the role of *RECQL4* in AKT mediated YB1 phosphorylation. Immunofluorescent staining results showed that p-YB1 in nuclear was substantially enhanced in *RECQL4*-induced MGC-803/Tet-on cells (Fig. 4A), whereas it was significantly decreased in *RECQL4*-suppressed AGS cells (Fig. 4B), suggesting that *RECQL4* regulates YB1 phosphorylation and its subsequent recruitment into the nuclear compartment. Consistently, Western blotting analysis showed an increased p-YB1 level in *RECQL4*-induced MGC-803/Tet-on cells (Fig. 4A). Likewise, *RECQL4* suppression in AGS cells resulted in a reduction in YB1 phosphorylation (Fig. 4B). However, AKT phosphorylation was unaffected either by *RECQL4* forced expression or suppression indicating that *RECQL4* performs its functions just downstream of AKT. Inhibition of AKT phosphorylation by treating the above cells with 1 μM of MK-2206 (a p-AKT inhibitor) for 2 h specifically abolished YB1 phosphorylation (Fig. 4A and 4B). This finding together with an elevated YB1-AKT interaction by the increased RECQL4 protein input (Fig. 3E) suggests that RECQL4 promotes AKT-mediated YB1 phosphorylation probably through facilitating the recruitment of YB1 to AKT by some unknown mechanism.

RECQL4 status affects the expression of YB1-targeted genes

We next wished to verify whether or not *RECQL4* affects the expression of YB1-targeted genes such as *MDR1* and *MVP* (26, 30) through modulating p-YB1

level. To this aim, we employed real-time RT-PCR to quantify the mRNA levels of a list of drug-resistance related genes, including *MDR1*, *MRP1-MRP4*, *BCRP* and *MVP*. The primer sets for a list of drug resistance-related genes was listed in Supplementary Table S4. As shown in Figure 5A, only two of the YB1 targeted genes, *MDR1* and *MVP*, were markedly up-regulated upon *RECQL4* induction in MGC-803/Tet-on/Flag-RECQL4 cells. Elevated MDR1 and MVP proteins upon *RECQL4* induction was validated by Western blotting (Fig. 5A). We further tested MDR1 and MVP protein levels in GC cell lines with varying expression levels of *RECQL4*. Consistently, cell lines with high *RECQL4* expression (AGS, HGC-27, NCI-N87, SNU-16) had a much higher *MDR1* at both mRNA and protein levels relative to cell lines with lower *RECQL4* expression (MGC-803, MKN45, and SNU-1, Fig. 5B). Three GC cell lines (AGS, NCI-N87, SNU-16) with high *RECQL4* expression also have a higher *MVP* expression at both mRNA and protein levels. HGC-27 cells were found to be an exception with low *MVP* expression despite a high endogenous *RECQL4* expression (Fig. 5C). Consistent with the potentiation of YB1 phosphorylation by RECQL4, expression of *YB1* target genes was also enhanced as a function of *RECQL4* expression.

RECQL4 regulates _MDR1_ expression in a YB1-dependent manner

First, *MDR1* expression was quantified by real-time RT-PCR in *RECQL4*-suppressed AGS cells with or without *YB1* suppression. As shown in Figure 6A, suppression of either *YB1* or *RECQL4* led to a decreased *MDR1*

expression, whereas no synergistic effect was observed with simultaneous silencing of both YB1 and RECQL4. Luciferase reporter assay was then employed in a reconstituted system to determine whether or not regulation of *MDR1* expression by RECQL4 is dependent on YB1. Native *YB1* was first silenced in MGC-803/Tet-on/Flag-RECQL4 cells by adenovirus-mediated *YB1* shRNA. *MDR1* promoter reporter plasmid was then co-transfected with *YB1*-expressing plasmid with or without *RECQL4* induction. Luciferase activities were measured at 72 h post transfection. As shown in Fig. 6B, *MDR1* promoter activity was at a very low level in *YB1*-silenced cells, however, it was markedly increased by about 5-fold after YB1 reconstitution. Additionally, only *RECQL4* induction in *YB1*-suppressed cells failed to activate the *MDR1* promoter. In contrast, reconstitution of both RECQL4 and YB1 significantly increased the *MDR1* promoter activity in relative to *YB1* reconstitution or RECQL4 induction only (Fig. 6B). p-AKT inhibition by treating the cells with 1 μM of MK-2206 (a p-AKT inhibitor) for 2 h specifically abolished the YB1 phosphorylation and subsequent *MDR1* activation even in the presence of *RECQL4* induction. These results convincingly demonstrate that *MDR1* expression is dependent on *RECQL4*-mediated transactivation potential of YB1. As with *MDR1* promoter, *MVP* promoter activation was also observed by a luciferase reporter assay upon reconstitution of either YB1 alone or YB1 and RECQL4 in *YB1*-silenced MGC-803/Tet-on/Flag-RECQL4 cells (Supplementary Fig. S7), suggesting that both of *MDR1* and *MVP* are downstream of RECQL4-YB1 signal pathway.

We further carried out *in vitro* electrophoretic mobility shift (EMSA) assay and

demonstrated both a direct binding of YB1 protein and a YB1-dependent binding of RECQL4 protein to *MDR1* promoter (Supplementary Fig. S8). To evaluate the binding efficiency of YB1 to *MDR1* promoter, a quantitative PCR-based chromatin immunoprecipitation (ChIP) assay was performed in MGC-803/Tet-on/Flag-RECQL4 cells. As shown in Figure 6C, YB1 binding to *MDR1* promoter was increased by over 7-fold when *RECQL4* was induced, further pointing to the critical role of *RECQL4* in regulating YB1 and MDR1 activation.

RECQL4 expression level governs cellular sensitivity to cisplatin

We next determined whether or not cisplatin sensitivity is altered after modulating *RECQL4* expression in GC cells. As shown in Figure 7A, forced *RECQL4* expression in GC cells (MKN45, SNU-1 and MGC-803) led to an increased level of MDR1, MVP and p-YB1, and consequently, a significantly higher cellular viability after cisplatin treatment when compared with their controls. Conversely, both a suppressed level of MDR1, MVP and p-YB1, and a significantly decreased cellular viability were observed after RECQL4 suppression in NCI-N87 and AGS cells when exposed to different concentrations of cisplatin (Fig. 7B). *RECQL4* Suppression in HGC-27 cells led to reduced p-YB1 and MDR1 levels as expected but MVP level was not altered, suggesting that RECQL4-YB1-MDR1 axis is critical for cisplatin sensitivity. The findings also imply that the role of *MVP* in drug sensitivity is not essential yet all the responding cells with exception of HGC-27 show a positive correlation between MVP expression level and drug sensitivity modulated by *RECQL4*.

Discussion

The most commonly used treatment regimen in gastric cancer is cisplatin-based chemotherapy (28), however, many gastric cancer patients have cancer recurrence after initial therapy and become refractory to chemotherapy following treatment. Thus, acquisition of cisplatin resistance is a major clinical obstacle for successful treatment of gastric cancer. However, the molecular basis for cisplatin resistance in GC is not clearly understood. In this study, we have presented a number of novel features that suggest prognostic and therapeutic significance of *RECQL4* in GC: (I) increased expression in GC cell lines and primary clinical samples; (II) correlation between high cytoplasmic or nuclear/cytoplasmic expression of *RECQL4* with poor survival of GC patients; (III) correlation between high *RECQL4* expression with cisplatin resistance; (IV) identification of physical and functional interaction of RECQL4 with a major transcription factor YB1; (V) promotion of RECQL4 mediated YB1 phosphorylation by AKT and (VI) transcriptional activation of a multidrug resistance gene *MDR1* by YB1 is regulated by *RECQL4* expression.

We have utilized 7 different GC cells lines in this study, whose genetic makeup is expected to be different from one another. Further, mutational spectrum of genes as well as the number of genes mutated may also considerably vary. These intrinsic features may influence their cellular phenotypes *in vitro* especially when these cells are challenged by exogenous DNA damage causing agents like cisplatin. In spite of the intrinsic variations, a reasonably good correlation between *RECQL4* expression

and cisplatin sensitivity was observed in most of the GC cell lines used in this study. Although cisplatin resistance was only marginally increased by forced *RECQL4* expression in some of the GC cell lines with low endogenous *RECQL4* expression, the acquired resistance was found to be statistically significant. It is likely that other unidentified mechanism(s) independent of *RECQL4* may also contribute to chemo resistance phenotype in GC cells.

Demonstration of a physical interaction, for the first time in this study between RECQL4 and YB1 indicates the functional significance of *RECQL4* upregulation in carcinogenic process (31, 32). *YB1* is an oncogenic transcription/translation factor that is overexpressed in a number of cancer types, and is frequently associated with poor outcome and chemotherapy resistance (27, 33). Being a substrate of AKT, YB1 can be phosphorylated at serine 102 by AKT, which is required for YB1 nuclear translocation in cancer cells (28, 34). In support, we found that RECQL4 substantially enhances the interaction between AKT and YB1 resulting in an increased level of p-YB1, illustrating a functional link between *RECQL4* overexpression and YB1 activation. Moreover, our data suggest that *RECQL4* functions just downstream of AKT and modulates AKT-dependent YB1 phosphorylation possibly by forming a functional complex with AKT through YB1.

Overexpression of the *MDR1* gene and corresponding P-glycoprotein (Pgp) efflux pumps is one of the best characterized MDR mechanisms, leading to resistance to a wide variety of anticancer agents in many types of human cancers (35-37). *MDR1* expression was shown to be regulated by transcription factors such as *YB1* (35).

Previous studies have illustrated a plausible association between *YB1* and drug resistance in both cultured cancer cells and clinical tumor samples (38, 39). However, there are certain gaps in our understanding with regard to how YB1 becomes activated to induce the expression of *MDR1* in cancer cells. Here, we provided evidence that induced expression of *RECQL4* in MGC-803/Tet-on/Flag-RECQL4 cells led to a markedly increased level of *MDR1* expression. In particular, a fair correlation between *RECQL4* status and MDR1 level was observed in GC cell lines tested. Moreover, ectopic expression of *RECQL4* in GC cells was observed to enhance the YB1 phosphorylation and further its nuclear translocation, and *vice versa*. The results of Luciferase reporter and ChIP-qPCR assays showed that *RECQL4* has the potential to modulate *MDR1* promoter activity by a *YB1*-dependent manner. This finding attributes an essential role to *RECQL4* in regulating the chemo resistance of GC cells through regulation of YB1-AKT-MDR1 downstream pathway.

Based on our findings, we suggest that *RECQL4* is a novel therapeutic target for GC and efficient *RECQL4* mediated targeting of AKT-YB1-MDR1 pathway is an effective treatment strategy for chemo sensitization of GC. Since *RECQL4* has demonstrated roles in DNA replication and repair (40, 41), *RECQL4* targeting may have additional advantages for cancer therapy.

References:

1. Shah MA. Update on metastatic gastric and esophageal cancers. J Clin Oncol 2015;33:1760-9.

2. Dasari S, Tchounwou PB. Cisplatin in cancer therapy: molecular mechanisms of action. Eur J Pharmacol 2014;740:364-78.
3. Kathawala RJ, Gupta P, Ashby CR Jr, Chen ZS. The modulation of ABC transporter-mediated multidrug resistance in cancer: A review of the past decade. Drug Resist Updat 2015;18:1-17.
4. Galluzzi L, Senovilla L, Vitale I, Michels J, Martins I, Kepp O, et al. Molecular mechanisms of cisplatin resistance. Oncogene 2012;31:1869-83.
5. Maginn EN, de Sousa CH, Wasan HS, Stronach EA. Opportunities for translation: targeting DNA repair pathways in pancreatic cancer. Biochim Biophys Acta 2014;1846:45-54.
6. Siddik ZH. Cisplatin: mode of cytotoxic action and molecular basis of resistance. Oncogene 2003;22:7265-79.
7. Xu X, Liu Y. Dual DNA unwinding activities of the Rothmund-Thomson syndrome protein, RECQ4. EMBO J 2009;28:568-77.
8. Petkovic M, Dietschy T, Freire R, Jiao R, Stagljar I. The human Rothmund-Thomson syndrome gene product, RECQL4, localizes to distinct nuclear foci that coincide with proteins involved in the maintenance of genome stability. J Cell Sci 2005;118:4261-9.
9. Croteau DL, Rossi ML, Canugovi C, Tian J, Sykora P, Ramamoorthy M, et al. RECQL4 localizes to mitochondria and preserves mitochondrial DNA integrity. Aging Cell 2012;11:456-66.
10. Wang JT, Xu X, Alontaga AY, Chen Y, Liu Y. Impaired p32 regulation caused by the lymphoma-prone RECQ4 mutation drives mitochondrial dysfunction. Cell Rep

2014;7:848-58.

11. Gupta S, De S, Srivastava V, Hussain M, Kumari J, Muniyappa K, et al. RECQL4 and p53 potentiate the activity of polymerase γ and maintain the integrity of the human mitochondrial genome. Carcinogenesis 2014;35:34-45.
12. Kitao S, Lindor NM, Shiratori M, Furuichi Y, Shimamoto A. Rothmund–thomson syndrome responsible gene, RECQL4: genomic structure and products. Genomics 1999;61:268-76.
13. Siitonen HA, Kopra O, Kaariainen H, Haravuori H, Winter RM, Saamanen AM, et al. Molecular defect of RAPADILINO syndrome expands the phenotype spectrum of RECQL diseases. Hum Mol Genet 2003; 12: 2837-44.
14. Van Maldergem L, Siitonen HA, Jalkh N, Chouery E, De Roy M, Delague V, et al. Revisiting the craniosynostosis-radial ray hypoplasia association: Baller-Gerold syndrome caused by mutations in the RECQL4 gene. J Med Genet 2006;43:148-52.
15. Wang LL, Gannavarapu A, Kozinetz CA, Levy ML, Lewis RA, Chintagumpala MM, et al. Association between osteosarcoma and deleterious mutations in the RECQL4 gene in Rothmund-Thomson syndrome. J Natl Cancer Inst 2003;95:669-74.
16. Jin W, Liu H, Zhang Y, Otta SK, Plon SE, Wang LL. Sensitivity of RECQL4-deficient fibroblasts from Rothmund-Thomson syndrome patients to genotoxic agents. Hum Genet 2008;123:643-53.
17. Santarpia L, Iwamoto T, Di Leo A, Hayashi N, Bottai G, Stampfer M, et al. DNA repair gene patterns as prognostic and predictive factors in molecular breast cancer subtypes. Oncologist 2013;18:1063-73.

18. Arora A, Agarwal D, Abdel-Fatah TM, Lu H, Croteau DL, Moseley P, et al. RECQL4 helicase has oncogenic potential in sporadic breast cancers. J Pathol 2016;238:495-501.
19. Maire G, Yoshimoto M, Chilton-MacNeill S, Thorner PS, Zielenska M, Squire JA. Recurrent RECQL4 imbalance and increased gene expression levels are associated with structural chromosomal instability in sporadic osteosarcoma. Neoplasia 2009;11:260-8.
20. Su Y, Meador JA, Calaf GM, Proietti De-Santis L, Zhao Y, Bohr VA, et al. Human RecQL4 helicase plays critical roles in prostate carcinogenesis. Cancer Res 2010;70:9207-17.
21. Fang H, Nie L, Chi Z, Liu J, Guo D, Lu X, et al. RecQL4 helicase amplification is involved in human breast tumorigenesis. PLoS One 2013;8:e69600.
22. Abdel-Fatah T, Arora A, Gorguc I, Abbotts R, Beebeejaun S, Storr S, et al. Are DNA repair factors promising biomarkers for personalized therapy in gastric cancer? Antioxid Redox Signal 2013;18:2392-8.
23. Storr SJ, Pu X, Davis J, Lobo D, Reece-Smith AM, Parsons SL, et al. Expression of the calpain system is associated with poor clinical outcome in gastro-oesophageal adenocarcinomas. J Gastroenterol 2013;48:1213-21.
24. Fareed KR, Al-Attar A, Soomro IN, Kaye PV, Patel J, Lobo DN, et al. Tumour regression and ERCC1 nuclear protein expression predict clinical outcome in patients with gastro-oesophageal cancer treated with neoadjuvant chemotherapy. Br J Cancer 2010;102:1600-7.
25. Rietveld CA, Esko T, Davies G, Pers TH, Turley P, Benyamin B, et al. Common genetic variants associated with cognitive performance identified using the proxy-phenotype

method. Proc Natl Acad Sci U S A 2014;111:13790-4.

26. Huang J, Tan PH, Li KB, Matsumoto K, Tsujimoto M, Bay BH. Y-box binding protein, YB-1, as a marker of tumor aggressiveness and response to adjuvant chemotherapy in breast cancer. Int J Oncol 2005;26:607-13.

27. Stein U, Bergmann S, Scheffer GL, Scheper RJ, Royer HD, Schlag PM, et al. YB-1 facilitates basal and 5-fluorouracil-inducible expression of the human major vault protein (MVP) gene. Oncogene 2005;24:3606-18.

28. Basaki Y, Hosoi F, Oda Y, Fotovati A, Maruyama Y, Oie S, et al. Akt-dependent nuclear localization of Y-box-binding protein 1 in acquisition of malignant characteristics by human ovarian cancer cells. Oncogene 2007;26:2736-46.

29. Bargou RC, Jurchott K, Wagener C, Bergmann S, Metzner S, Bommert K, et al. Nuclear localization and increased levels of transcription factor YB-1 in primary human breast cancers are associated with intrinsic MDR1 gene expression. Nat Med 1997;3:447-50.

30. Cunningham D, Allum WH, Stenning SP, Thompson JN, Van de Velde CJ, Nicolson M, et al. Perioperative chemotherapy versus surgery alone for resectable gastroesophageal cancer. N Engl J Med 2006;355:11-20.

31. Bergmann S, Royer-Pokora B, Fietze E, Jurchott K, Hildebrandt B, Trost D, et al. YB-1 provokes breast cancer through the induction of chromosomal instability that emerges from mitotic failure and centrosome amplification. Cancer Res 2005;65:4078-87.

32. Berquin IM, Min Y, Wu R, Wu H, Chen YQ. Expression signature of the mouse prostate. J Biol Chem 2005;280:36442-51.

33. Wu J, Stratford AL, Astanehe A, Dunn SE. YB-1 is a transcription/translation factor that

orchestrates the oncogenome by hardwiring signal transduction to gene expression. Transl Oncogenomics 2007;2:49-65.

34. Sutherland BW, Kucab J, Wu J, Lee C, Cheang MC, Yorida E, et al. Akt phosphorylates the Y-box binding protein 1 at Ser102 located in the cold shock domain and affects the anchorage-independent growth of breast cancer cells. Oncogene 2005;24:4281-92.
35. Labialle S, Gayet L, Marthinet E, Rigal D, Baggetto LG. Transcriptional regulators of the human multidrug resistance 1 gene: recent views. Biochem Pharmacol 2002;64:943-8.
36. Fu D, Arias IM. Intracellular trafficking of P-glycoprotein. Int J Biochem Cell Biol 2012;44:461-4.
37. Ueda K, Clark DP, Chen CJ, Roninson IB, Gottesman MM, Pastan I. The human multidrug resistance (mdr1) gene. cDNA cloning and transcription initiation. J Biol Chem 1987;262:505-8.
38. Chatterjee M, Rancso C, Stuhmer T, Eckstein N, AndruliS M, Gerecke C, et al. The Y-box binding protein YB-1 is associated with progressive disease and mediates survival and drug resistance in multiple myeloma. Blood 2008;111:3714-22.
39. Janz M, Harbeck N, Dettmar P, Berger U, Schmidt A, Jurchott K, et al. Y-box factor YB-1 predicts drug resistance and patient outcome in breast cancer independent of clinically relevant tumor biologic factors HER2, uPA and PAI-1. Int J Cancer 2002;97:278-82.
40. Liu Y. Rothmund-Thomson syndrome helicase, RECQ4: On the crossroad between DNA replication and repair. DNA Repair (Amst) 2010;9:325-30.

41. Singh DK, Karmakar P, Aamann M, Schurman SH, May A, Croteau DL, et al. The involvement of human RECQL4 in DNA double-strand break repair. Aging Cell 2010; 9: 358-71.

Figure Legends:

Figure 1. RECQL4 expression in clinical gastric cancer (GC) specimens. (A) RECQL4 mRNA level determined by quantitative real time PCR in normal gastric tissues and GC specimens with different pathological grades (TissueScan cDNA array, Origene). Normal gastric and cancer specimens were marked with asterisks (*). Other unmarked samples were esophageal tissue specimens. The values represent mean ± SD from three independent experiments. (B) RECQL4 protein level in 11 pairs of human GC (T) and matched normal gastric controls (N) determined by Western blotting using RECQL4 antibody from Novus Biologicals. (C) Microphotographs of RECQL4 protein expression in gastric adenocarcinomas. RECQL4 antibody from Novus Biologicals was used for IHC staining. **(**D**)** Kaplan Meier curves showing disease specific survival based on RECQL4 protein expression in different cellular compartments.

Figure 2. RECQL4 expression level affects sensitivity to cisplatin treatment. (A)RECQL4 protein level in GC cell lines determined by Western blotting using RECQL4 antibody from Novus Biologicals. (B) Viability of GC cells after treatment with graded concentrations of cisplatin for 72 h was quantified by MTT assay with

10 duplicated wells for each time-point of each cell line. The values represent mean ± SD from three independent experiments.

Figure 3. RECQL4 physically interacts with YB1. (A) Endogenous YB1 and AKT were detected in anti-Flag immunoprecipitates against Flag-RECQL4. Flag-GFP immunoprecipitates were used as negative controls. (B) Endogenous RECQL4 and AKT were detected in anti-YB1 (Cell Signaling) immunoprecipitates determined by Western blotting analysis. (C) Direct interaction between RECQL4 and YB1, and (D) indirect interaction between RECQL4 and AKT were demonstrated by *in vitro* pull-down assay. (E) An enhanced interaction between AKT and YB1 was observed upon an increased input of RECQL4 protein (antibody from Cell signaling). The pull-down YB1 protein was quantified using the Image J software (http://rsbweb.nih.gov/ij/) and normalized to AKT loading control.

Figure 4. RECQL4 potentiates YB1 phosphorylation in an AKT-dependent manner. Level of p-YB1 determined by immunofluorescent staining and Western blotting analysis in: (A) MGC-803/Tet-on/Flag-RECQL4 cells upon RECQL4 induction and (B) AGS cells upon adenovirus-mediated RECQL4 silencing with or without treatment of AKT inhibitor-MK-2206. RECQL4 antibody from Novus Biologicals was used. Images were captured by Leica TCS SP5 Confocal microscope. Fluorescent staining of p-YB1 in nucleus was quantified by Image J software (http://imagej.net/Welcome). At least 200 cells were analyzed for each sample.

Values represent the mean ± SD.

Figure 5. RECQL4 modulates MDR1 expression. (A) The relative mRNA levels of a list of drug resistance-related genes were quantified by real time RT-PCR in MGC-803/Tet/on/Flag-RECQL4 cells after RECQL4 induction. Levels of MDR1, MVP, p-YB1 and p-AKT proteins were examined by Western blotting. (B) Expression of MDR1 (B) and MVP (C) at both mRNA and protein levels in GC cell lines determined by quantitative real time RT-PCR and Western blotting analyses. RECQL4 antibody was from Novus Biologicals; MDR1 (Cat. ab129450) and MVP (Cat. ab175239) antibodies were from Abcam.

Figure 6. RECQL4 regulates MDR1 in a YB1-dependent manner. (A) MDR1 expression was quantified by real time RT-PCR in AGS cells after YB1 and/ RECQL4 suppression. RECQL4 antibody from Cell Signaling was used. (B) Effect of YB1 and RECQL4 on MDR1 promoter activity determined by a reconstitution assay in MGC-803/Tet-on/Flag-RECQL4 cells. Protein levels of RECQL4 (antibody from Novus Biologicals), p-YB1 and p-AKT as well as relative luciferase activity were then determined. (C) YB1 binding ability to MDR1 promoter region was quantified by a PCR-based ChIP assay. Values represent the mean ± SD from three independent experiments.

Figure 7. Altered **s**ensitivity to cisplatin by modulating RECQL4 expression.

RECQL4 expression was reconstituted in MKN45, SNU-1, MGC-803 cells (A) or suppressed in NCI-N87, AGS, HGC-27 cells (B). Levels of RECQL4, MDR1, MVP and p-AKT proteins were determined by Western blotting. RECQL4 antibody from Novus Biologicals was used. Cellular viability after treatment with graded concentrations of cisplatin was quantified by MTT assay. The data in the curves represent mean ± SD from three independent experiments. Student' t-test was used for statistical analysis.

Figure 1

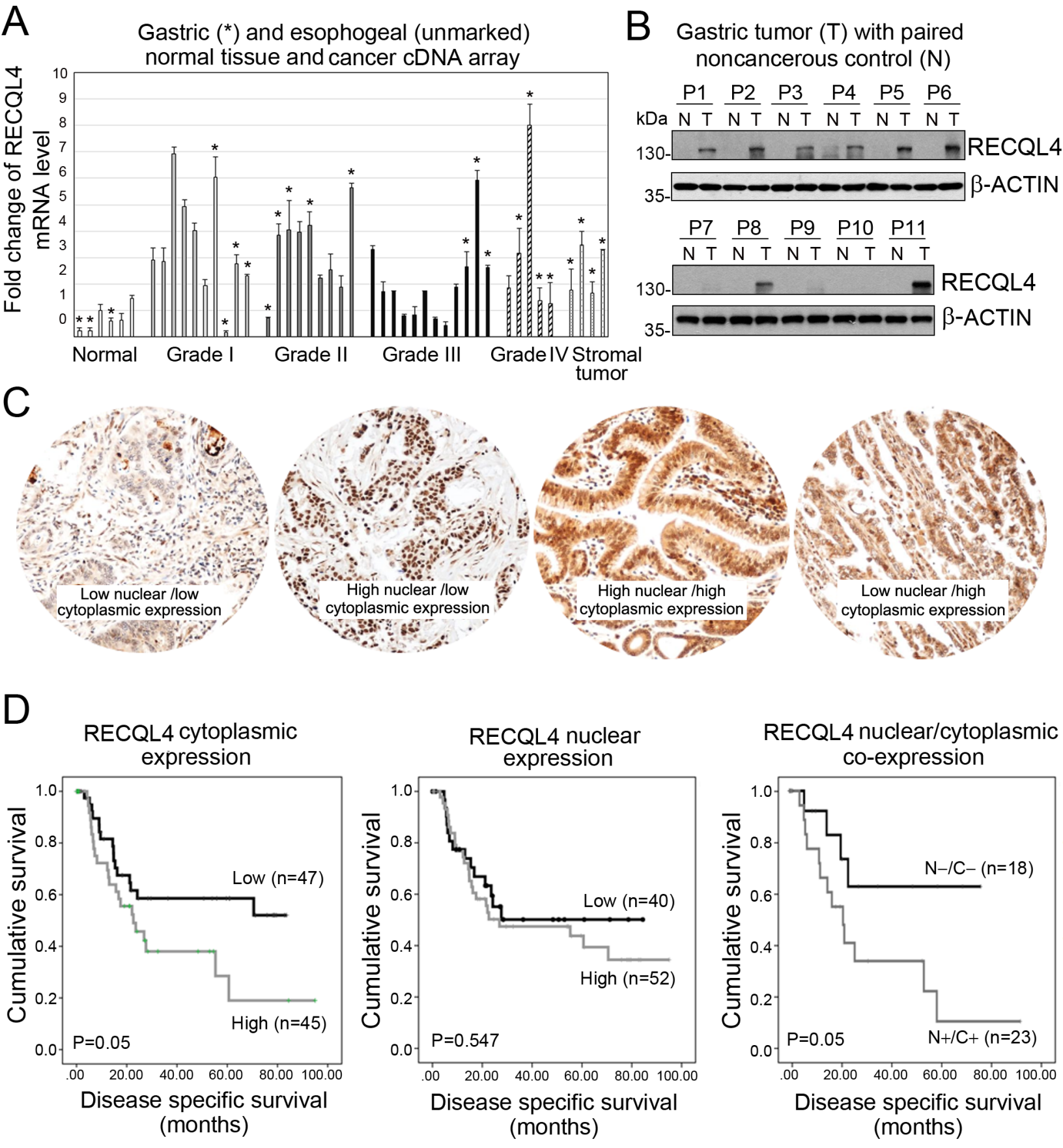
A
Gastric (*) and esophogeal (unmarked) normal tissue and cancer cDNA array
Fold change of RECQL4 mRNA level
Normal
Grade I
Grade II
Grade III
Grade IV
Stromal tumor
B
Gastric tumor (T) with paired noncancerous control (N)
P1 P2 P3 P4 P5 P6
kDa N T N T N T N T N T N T
130-
RECQL4
35-
β-ACTIN
P7 P8 P9 P10 P11
N T N T N T N T N T
130-
RECQL4
35-
β-ACTIN
C
Low nuclear /low cytoplasmic expression
High nuclear /low cytoplasmic expression
High nuclear /high cytoplasmic expression
Low nuclear /high cytoplasmic expression
D
RECQL4 cytoplasmic expression
Cumulative survival
Low (n=47)
High (n=45)
P=0.05
Disease specific survival (months)
RECQL4 nuclear expression
Cumulative survival
Low (n=40)
High (n=52)
P=0.547
Disease specific survival (months)
RECQL4 nuclear/cytoplasmic co-expression
Cumulative survival
N–/C– (n=18)
N+/C+ (n=23)
P=0.05
Disease specific survival (months)

Figure 2

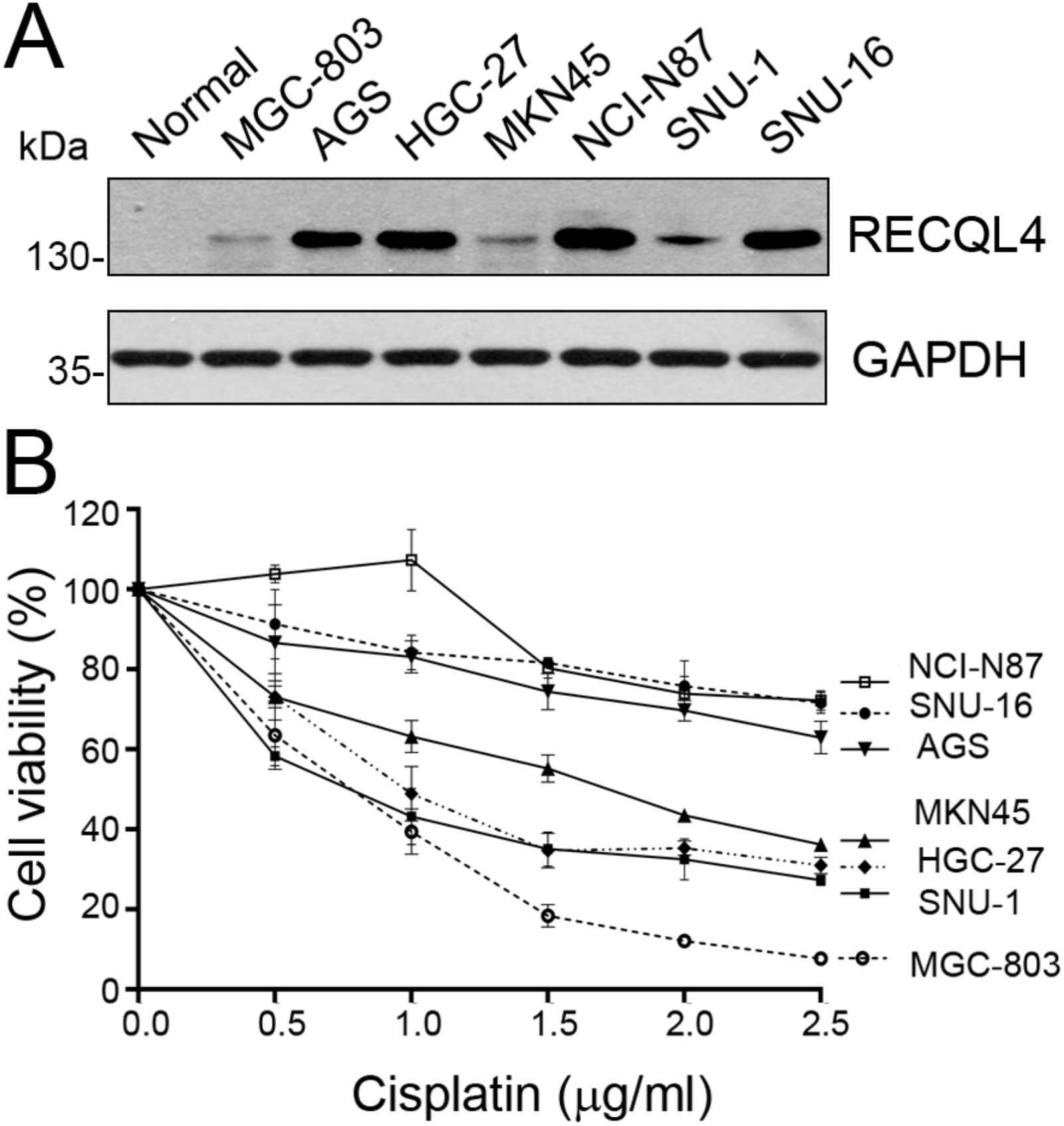
A
Normal
MGC-803
AGS
HGC-27
MKN45
NCI-N87
SNU-1
SNU-16
kDa
130-
RECQL4
35-
GAPDH
B
Cell viability (%)
120
100
80
60
40
20
0
0.0
0.5
1.0
1.5
2.0
2.5
Cisplatin (μg/ml)
NCI-N87
SNU-16
AGS
MKN45
HGC-27
SNU-1
MGC-803

Figure 3

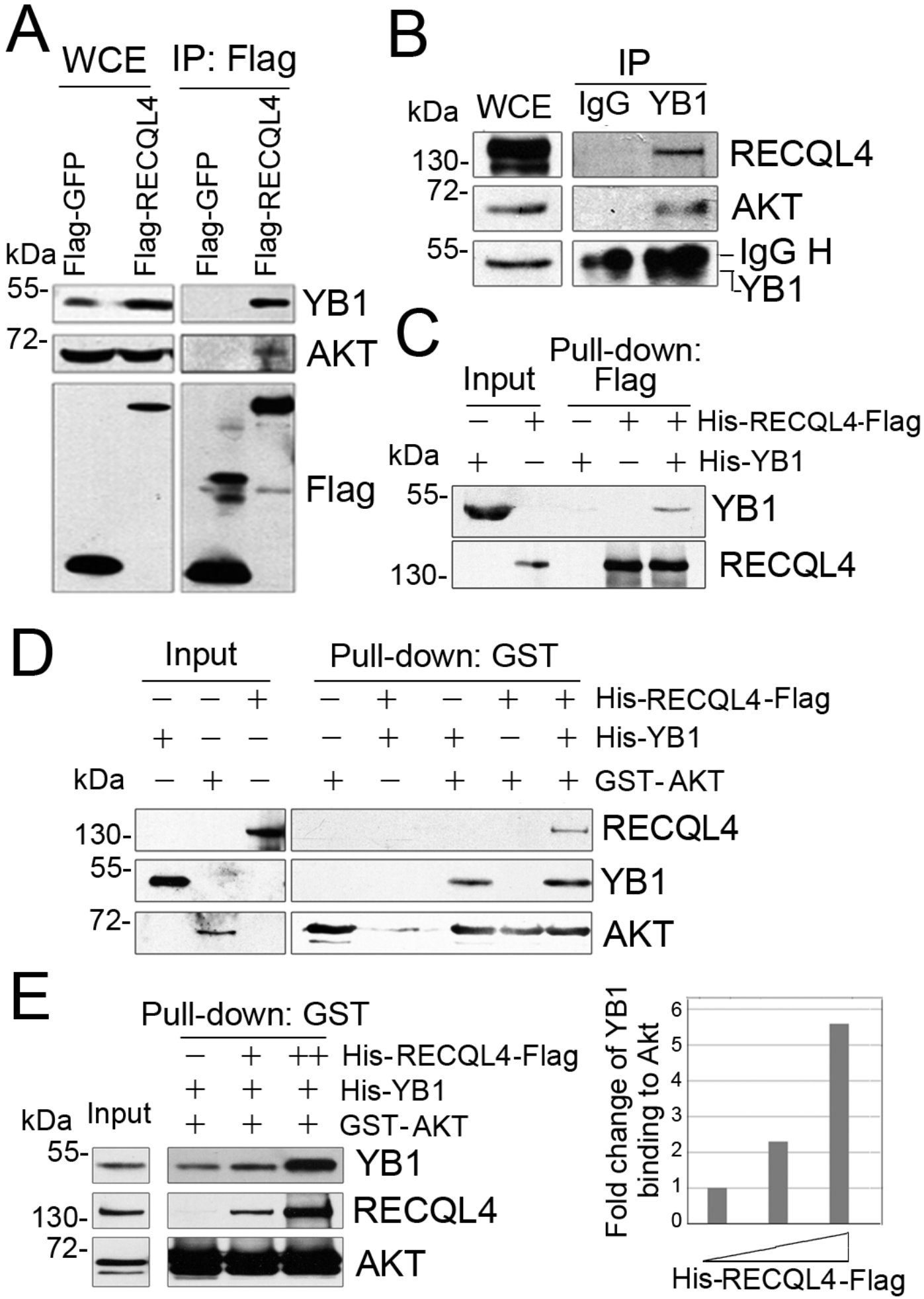
A
WCE
IP: Flag
Flag-GFP
Flag-RECQL4
Flag-GFP
Flag-RECQL4
kDa
55-
72-
YB1
AKT
Flag
B
IP
kDa
WCE
IgG
YB1
130-
72-
55-
RECQL4
AKT
IgG H
YB1
C
Pull-down:
Input
Flag
His-RECQL4-Flag
His-YB1
kDa
55-
130-
YB1
RECQL4
D
Input
Pull-down: GST
His-RECQL4-Flag
His-YB1
GST-AKT
kDa
130-
55-
72-
RECQL4
YB1
AKT
E
Pull-down: GST
His-RECQL4-Flag
His-YB1
GST-AKT
kDa
Input
55-
130-
72-
YB1
RECQL4
AKT
Fold change of YB1 binding to Akt
0
1
2
3
4
5
6
His-RECQL4-Flag

Figure 4

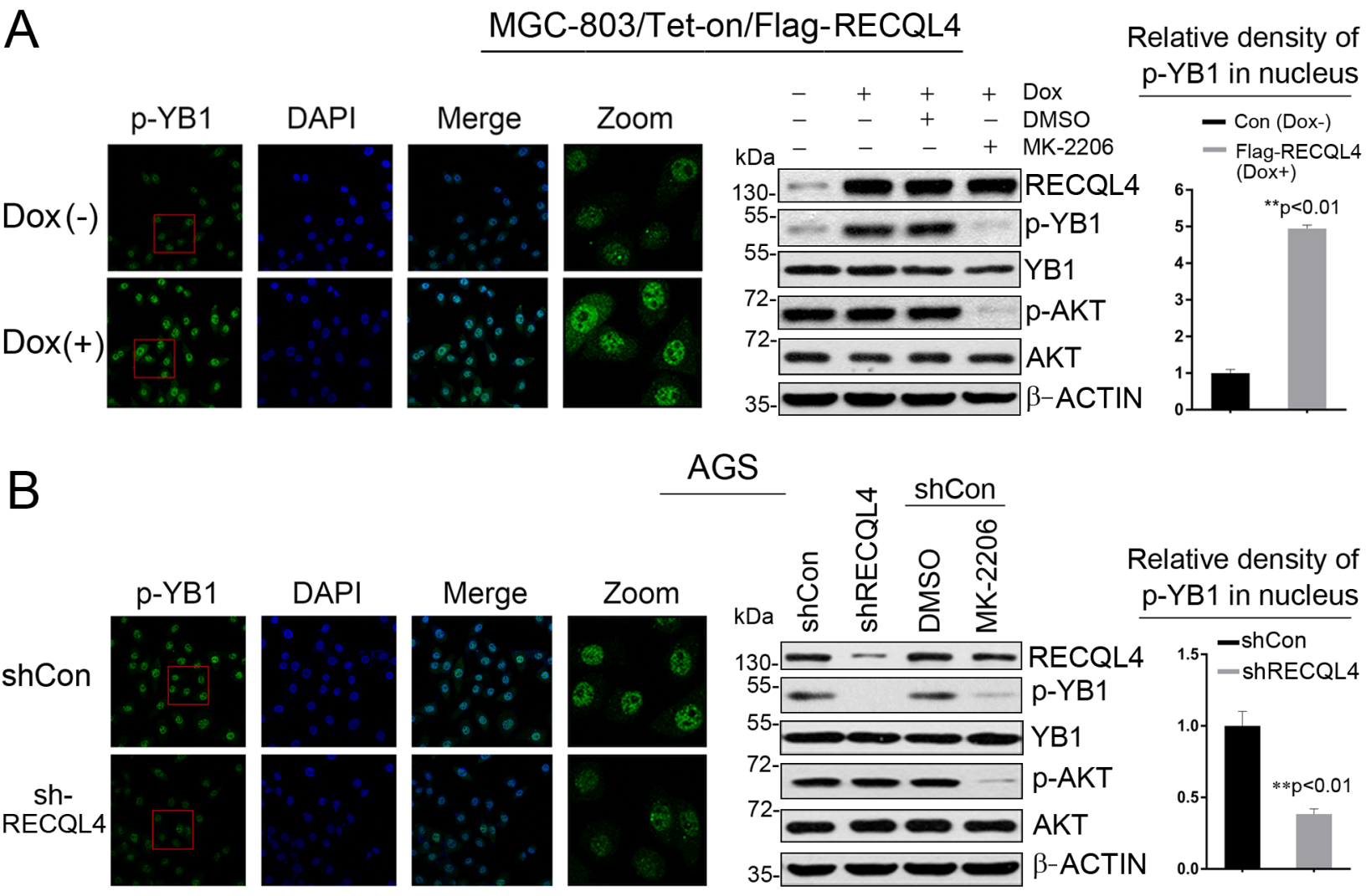
A
MGC-803/Tet-on/Flag-RECQL4
p-YB1
DAPI
Merge
Zoom
Dox(-)
Dox(+)
Dox
DMSO
MK-2206
kDa
130-
55-
55-
72-
72-
35-
RECQL4
p-YB1
YB1
p-AKT
AKT
β-ACTIN
Relative density of p-YB1 in nucleus
Con (Dox-)
Flag-RECQL4 (Dox+)
**p<0.01
B
AGS
shCon
shRECQL4
DMSO
MK-2206
sh-RECQL4
Relative density of p-YB1 in nucleus
shCon
shRECQL4
**p<0.01

Figure 5

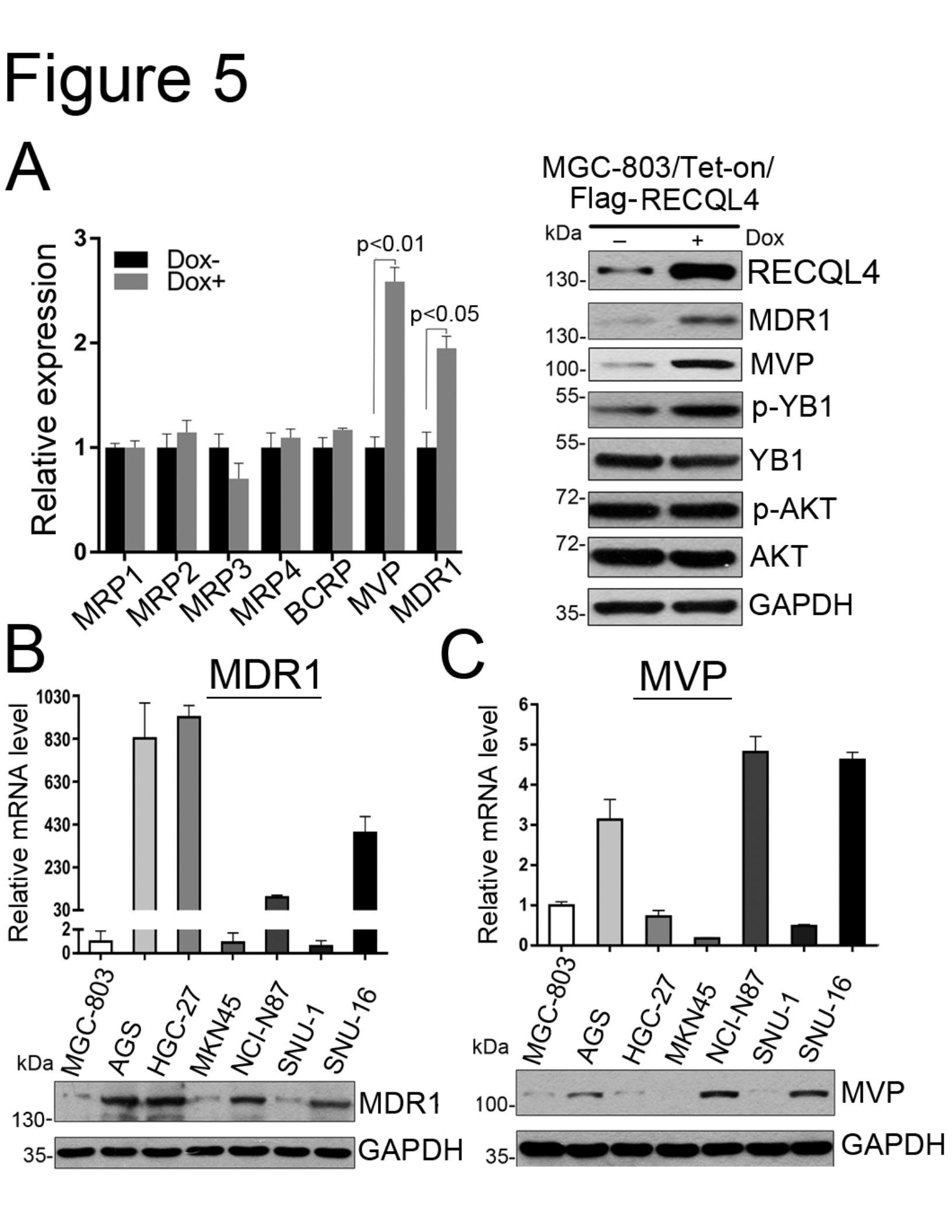
A
MGC-803/Tet-on/
Flag-RECQL4
Relative expression
Dox-
Dox+
p<0.01
p<0.05
MRP1
MRP2
MRP3
MRP4
BCRP
MVP
MDR1
kDa
–
+
Dox
RECQL4
MDR1
MVP
p-YB1
YB1
p-AKT
AKT
GAPDH
B
MDR1
Relative mRNA level
MGC-803
AGS
HGC-27
MKN45
NCI-N87
SNU-1
SNU-16
C
MVP
Relative mRNA level

Figure 6

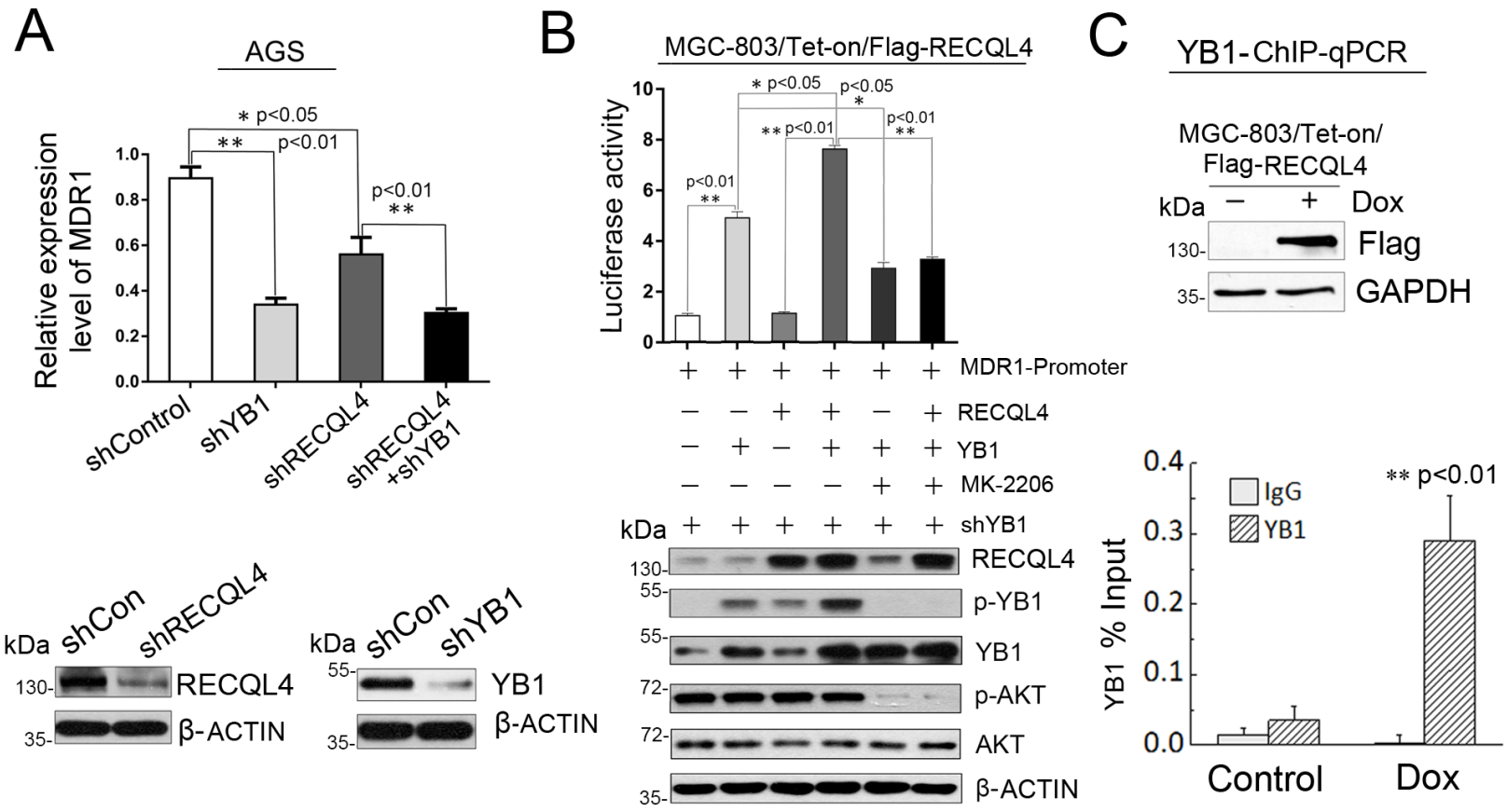
A
AGS
Relative expression level of MDR1
* p<0.05
** p<0.01
p<0.01
**
shControl
shYB1
shRECQL4
shRECQL4 +shYB1
kDa
shCon
shRECQL4
130-
RECQL4
35-
β-ACTIN
kDa
shCon
shYB1
55-
YB1
35-
β-ACTIN
B
MGC-803/Tet-on/Flag-RECQL4
Luciferase activity
* p<0.05
p<0.05
** p<0.01
p<0.01
p<0.01
**
MDR1-Promoter
RECQL4
YB1
MK-2206
shYB1
kDa
130-
RECQL4
55-
p-YB1
55-
YB1
72-
p-AKT
72-
AKT
35-
β-ACTIN
C
YB1-ChIP-qPCR
MGC-803/Tet-on/ Flag-RECQL4
kDa
Dox
130-
Flag
35-
GAPDH
YB1 % Input
IgG
YB1
** p<0.01
Control
Dox

Figure 7

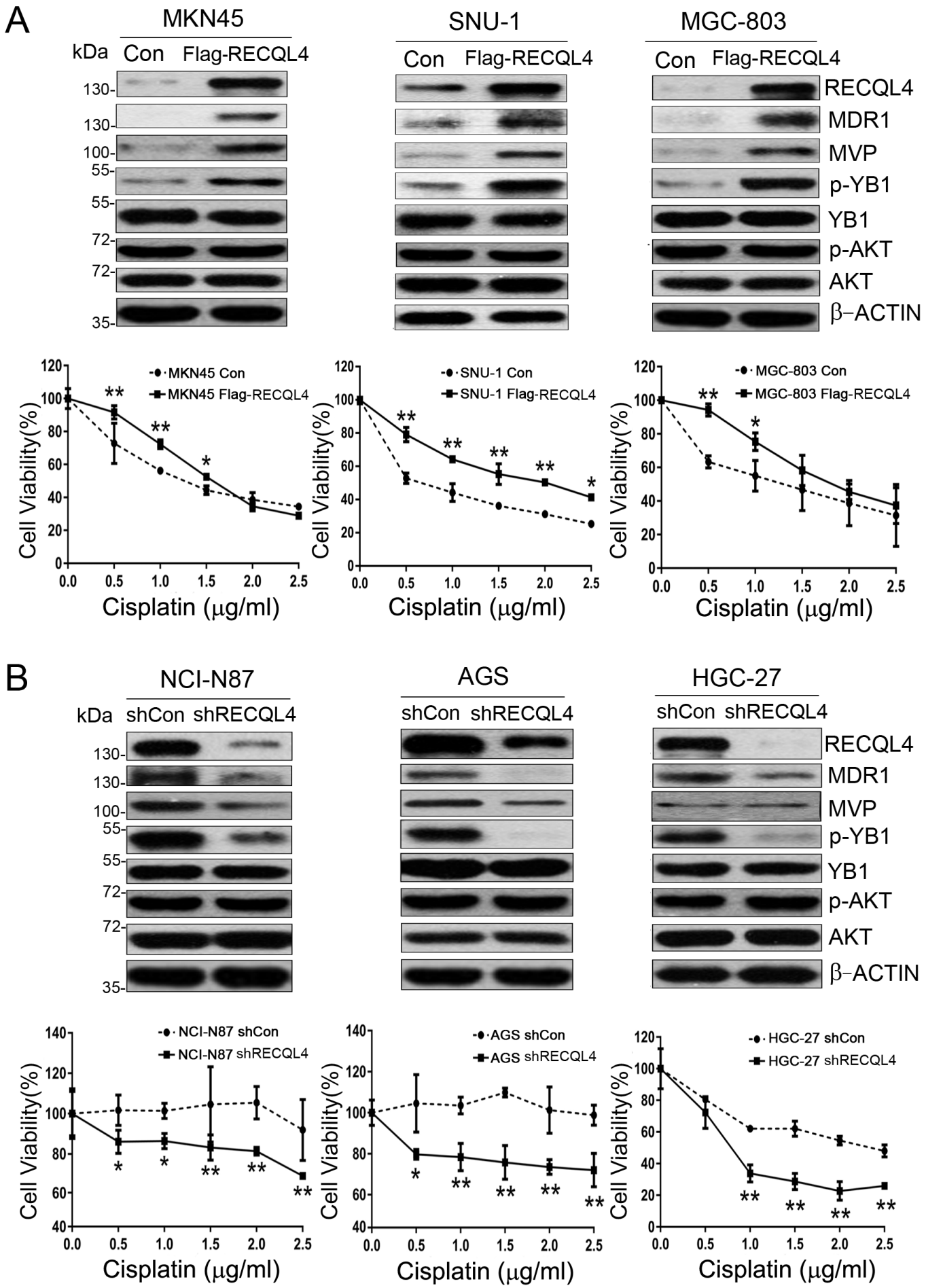
A
MKN45
SNU-1
MGC-803
kDa
Con
Flag-RECQL4
130-
130-
100-
55-
55-
72-
72-
35-
RECQL4
MDR1
MVP
p-YB1
YB1
p-AKT
AKT
β-ACTIN
MKN45 Con
MKN45 Flag-RECQL4
SNU-1 Con
SNU-1 Flag-RECQL4
MGC-803 Con
MGC-803 Flag-RECQL4
Cell Viability(%)
Cisplatin (μg/ml)
B
NCI-N87
AGS
HGC-27
shCon
shRECQL4
NCI-N87 shCon
NCI-N87 shRECQL4
AGS shCon
AGS shRECQL4
HGC-27 shCon
HGC-27 shRECQL4

Contents of Supplementary Figures and Tables

1. **Supplementary Figure S1.** PCR-SSCP analysis of 21 exons of human RecQL4 gene in human gastric cancer cell lines.
2. **Supplementary Figure S2**. PCR-SSCP analysis of 21 exons of human RecQL4 gene in human primary gastric tumors and matched gastric tissue controls
3. **Supplementary Figure S3**. DNA sequencing result of exons 2-3 of human RecQL4 gene in AGS and HGC-27 cells.
4. **Supplementary Figure S4.** Coomassie brilliant blue staining images of purified tagged-proteins expressed in *E. Coli*.
5. **Supplementary Figure S5.** YB1 domains specifically interacting with RecQL4.
6. **Supplementary Figure S6**. Level of YB1 and Akt interaction in cytoplasmic(C) and nuclear (N) fractions from MGC-803/Tet-on/Flag-RecQL4 cells with or without RecQL4 induction.
7. **Supplementary Figure S7**. Effect of YB1 and RecQL4 on MVP promoter activity.
8. **Supplementary Figure S8**. *In vitro* direct binding of YB1 and/ RecQL4 proteins to MDR1 promoter region detected by EMSA analysis.
9. **Supplementary Table S1**. Clinicopathological characteristics of patients with early gastric adenocarcinomas
10. **Supplementary Table S2**. Correlation of RecQL4 nuclear and cytoplasmic expression with clinical parameters of gastric cancer patients
11. **Supplementary Table S3**. Primer sets of 21 exons of human RecQL4 gene used for PCR-SSCP analysis.
12. **Supplementary Table S4**. PCR primer sets of drug resistance related genes used for real time RT-PCR analysis

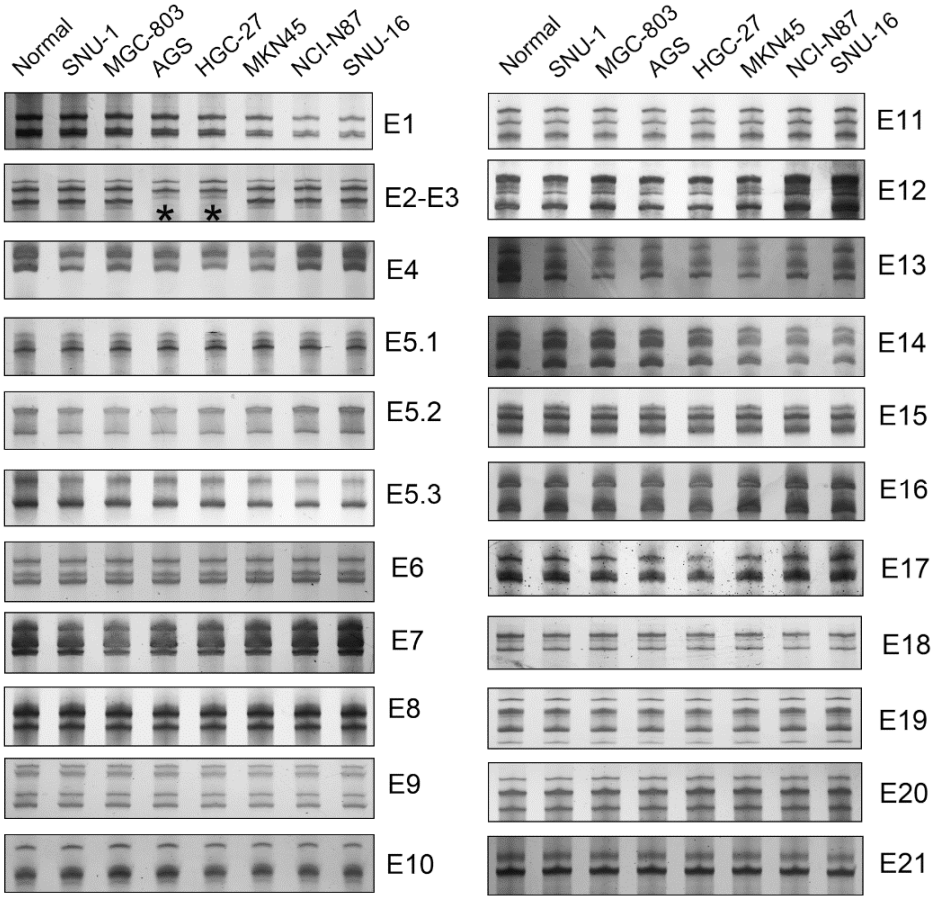

Supplementary Figure S1. PCR-SSCP analysis of 21 exons of human RecQL4 gene in huamn gastric tumor cell lines. “*” marked: abnormal bands revealed by SSCP.

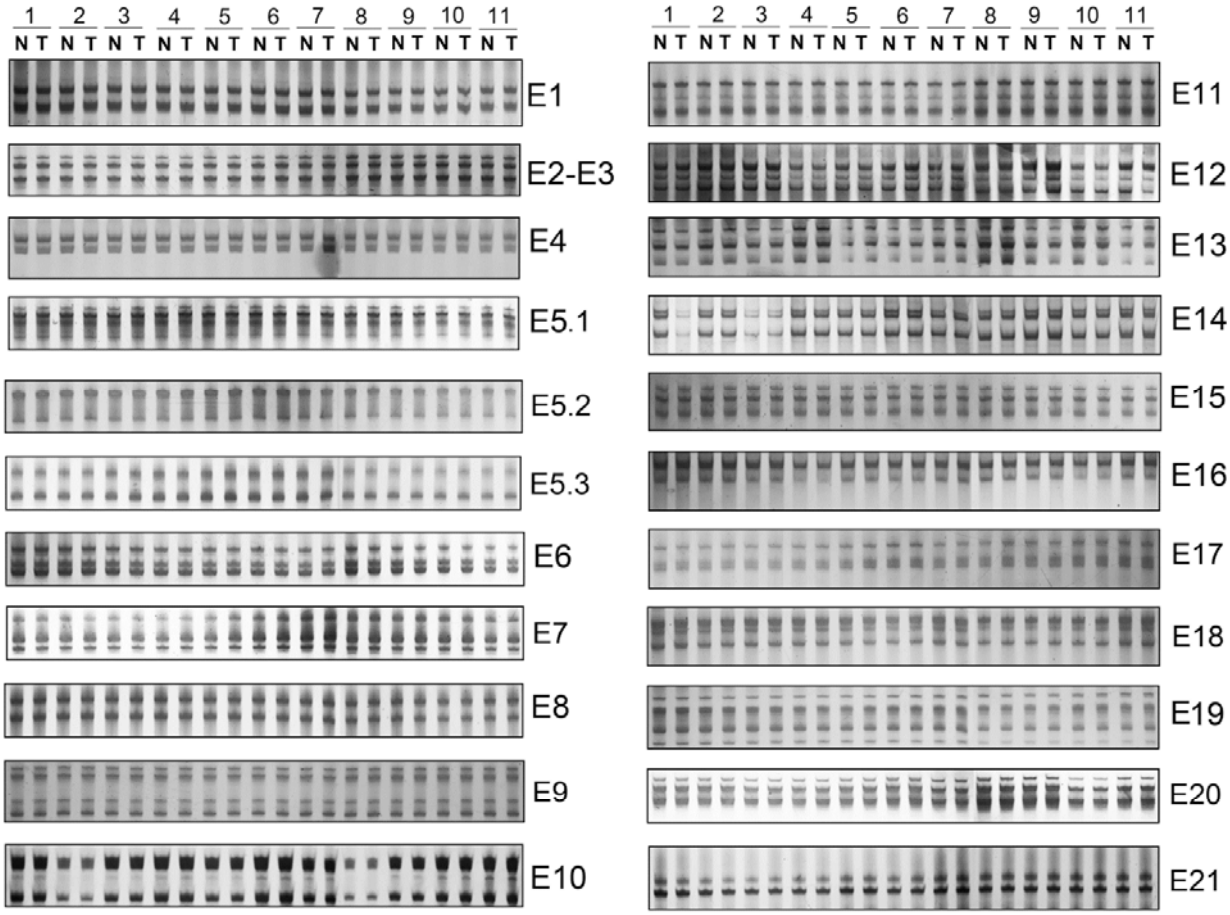

Supplementary Figure S2. PCR-SSCP analysis of 21 exons (E) of human RecQL4 gene in human primary gastric tumors (T) and matched normal gastric tissue controls (N). Exon 5 was divided into three fragments: E5.1, E5.2 and E5.3.

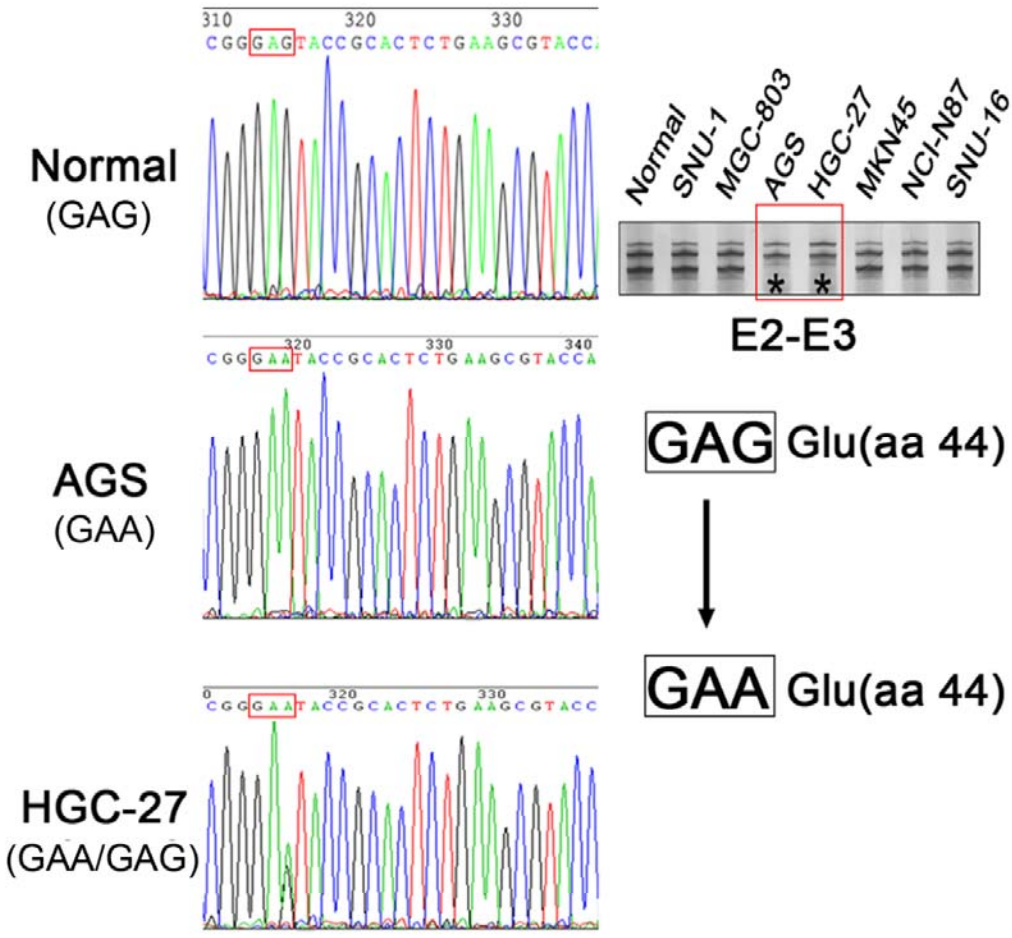

Supplementary Figure S3. DNA sequencing results of exons 2-3 of RecQL4 gene from AGS and HGC-27 cells. A synonymous mutation was demonstrated in AGS and HGC-27 cell lines. A double-peak in sequencing data of HGC-27 cells suggests that the mutation is heterogeneous.

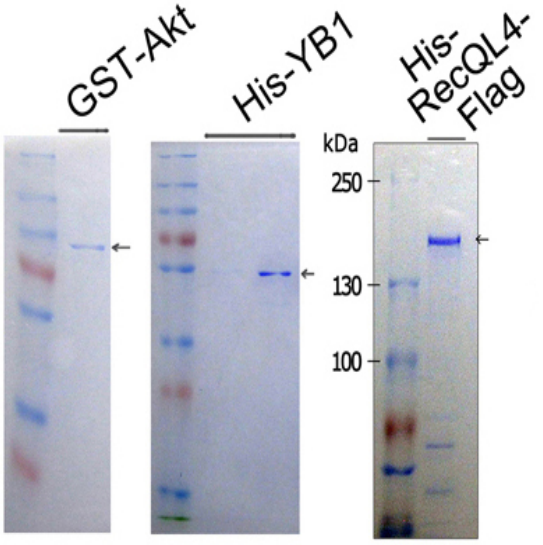

Supplementary Figure S4. Coomassie brilliant blue staining images of purified tagged-proteins expressed in *E.Coli.*

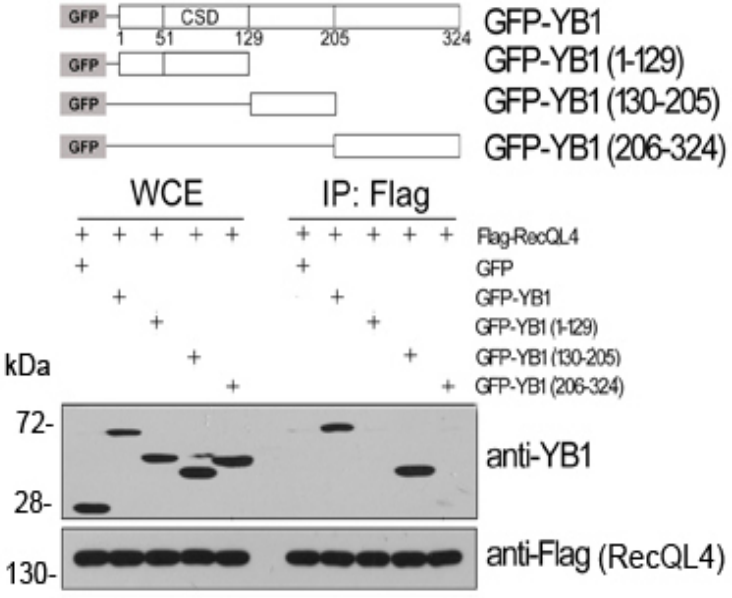

Supplemental Figure S5. YB1 domains specifically interacting with RecQL4, various GFP-YB1 constructs with deletion of different domains were generated. The YB1 fragment 130-205aa is responsible for the interaction with RecQL4

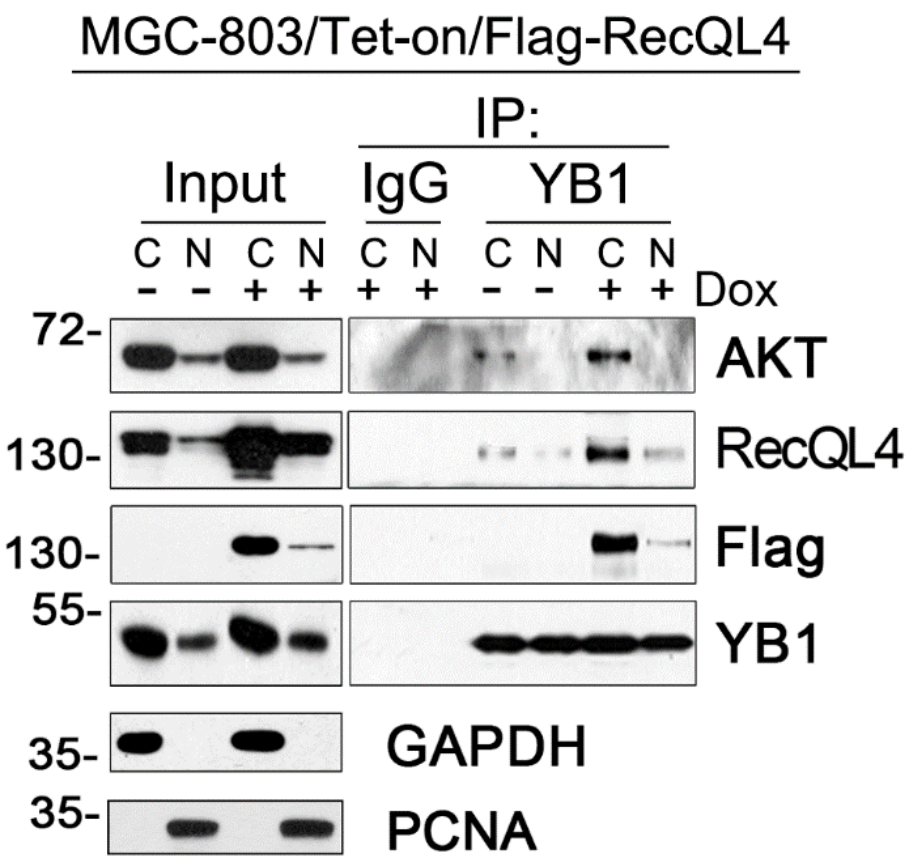

Supplementary Figure S6. Level of YB1 and Akt interaction in cytoplasmic (C) and nuclear (N) fractions from MGC-803/Tet-on/ Flag-RecQL4 cells with or without RecQL4 induction examined by IP and Western blotting analyses

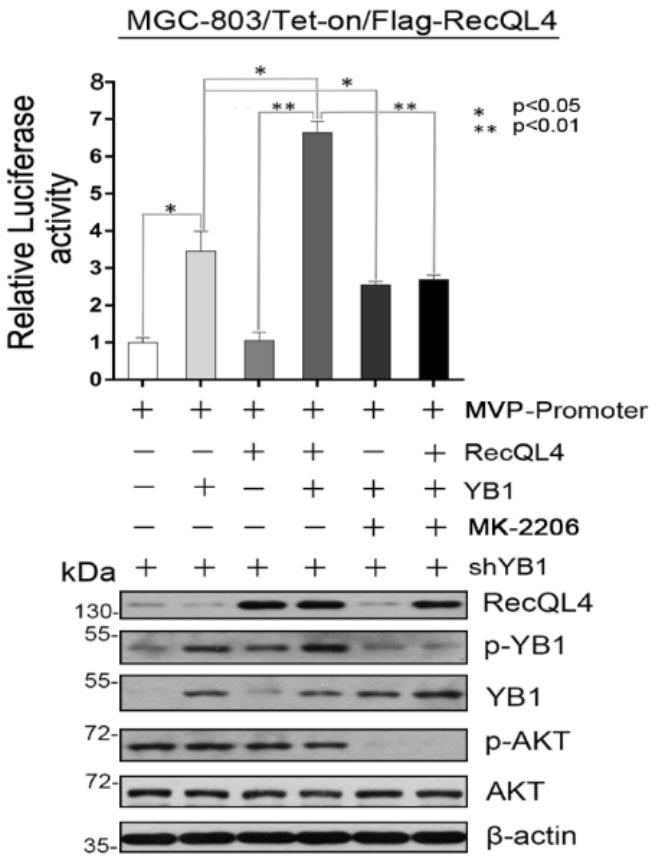

Supplementary Figure S7. Effect of YB1 and RecQL4 on MVP promoter activity. Native YB1 expression in MGC-803/Tet-on/Flag-RecQL4 was first silenced, and then a reconstitution assay was performed on YB1-silenced cells by transfecting YB1 plasmid concurrently with or without RecQL4 induction and addition of Akt inhibitor MK-2206. MVP gene promoter region (from-679 to +23) containing Y-box consensus sequence used for luciferase reporter assay was amplified by PCR. Primer pair: forward: 5'-ggggtaccCGTACCTGCT GGAGCCTGG-3', reverse: 5'-cccaagcttCCAGGCT CCAGCAGGTACG-3'. The PCR fragment were then cloned into the KpnI/HindIII sites of pGL3-Basic vector, and verified by sequencing.

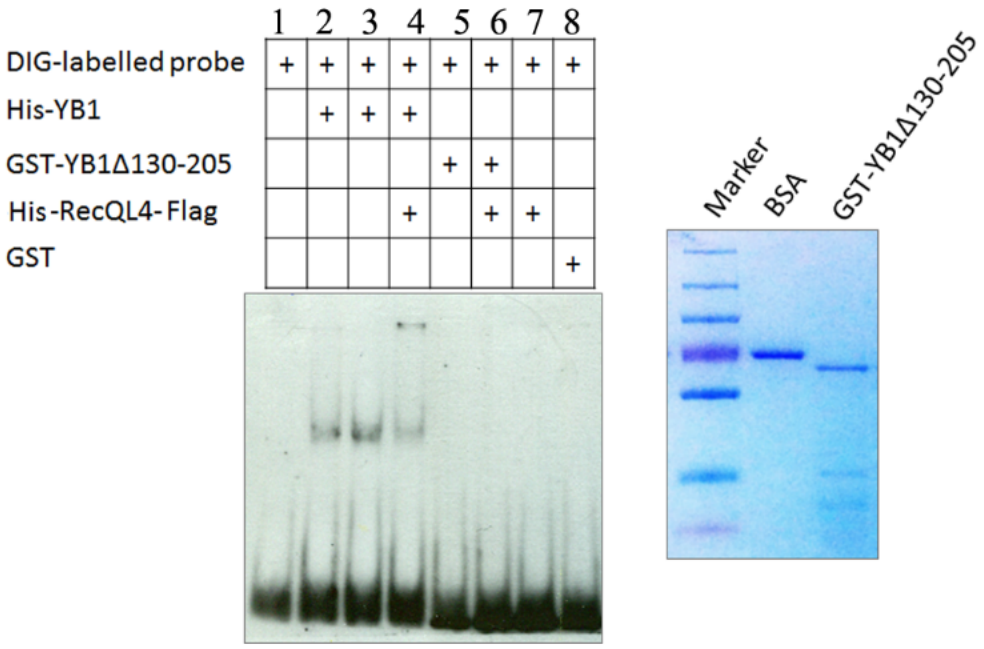

Supplementary Figure S8. In vitro direct binding of YB1 and/ RecQL4 protein to MDR1 promoter region detected by electrophoretic mobility shift assay (EMSA). YB1 protein can bind to the Digoxin (DIG)-labelled Y-box DNA probe of MDR1 promoter, which results in a shift band (lanes 2 & 3). Another supershift band was also observed when adding recombinant His-RecQL4-Flag protein in the reaction system (lane 4). YB1 mutant with deletion of the interaction domain with RecQL4 also losses the MDR1 promoter binding activity.

Supplementary Table S1: Clinicopathological characteristics of patients with early gastric adenocarcinomas (n=148)

Age (Median years)	74 (41-90)
Gender (M/F%)	74 / 26 %
Tumour site	Gastric – 87% GOJ – 12% Oesophageal – 1%
Grade (1-3)	1 – 9% 2 – 35% 3 – 56%
Tumour depth (T0-4)	T1 – 10% T2 – 33% T3 – 54% T4 – 3%
Nodal stage	N0 – 22% N1 – 52% N2 – 18% N3 – 8%
Vascular invasion (Y)	67%
Perineural invasion (Y)	45%
Status	Alive – 37% Dead – 63%

Supplementary Table S2: Correlation of RecQL4 Nuclear & Cytoplasmic expression with clinical parameters of gastric cancer patients

VARIABLE	RECQL4 Nuclear (Rn) & RECQL4 Cytoplasmic (Rc) Protein Co-expression				P-value
	Rn-/Rc- N (%)	Rn+/Rc- N (%)	Rn-/Rc+ N (%)	Rn+/Rc+ N(%)	
T Stage					
T1	3 (16.7)	1 (3.5)	3 (13.6)	1 (4.3)	0.485
T2	6 (33.3)	9 (31.0)	6 (27.3)	6 (26.1)	
T3	8 (44.4)	19 (65.5)	13 (59.1)	14 (60.9)	
T4	1 (5.6)	0 (0.0)	0 (0.0)	2 (8.7)	
Overall Stage					
Stage 1	2 (11.1)	1 (3.4)	3 (13.6)	1 (4.3)	0.332
Stage 2	7 (38.9)	11 (37.9)	6 (27.3)	6 (21.7)	
Stage 3	9 (50.0)	17 (58.7)	13 (59.1)	15 (65.3)	
Stage 4	0 (0.0)	0 (0.0)	0 (0.0)	2 (8.7)	
LN status					
Negative	6 (33.3)	6 (20.7)	6 (27.3)	2 (8.7)	0.247
Positive	12 (66.7)	23 (79.3)	16 (72.7)	21 (91.3)	
Tumour Grade					
G1/G2	10 (55.6)	6 (20.7)	8 (36.4)	12 (52.2)	**0.048**
G3	8 (44.4)	23 (79.3)	14 (63.6)	11 (47.8)	
CRM Involvement					
No	3 (75.0)	0 (0.0)	0 (0.0)	2 (33.3)	**0.041**
Yes	1 (25.0)	4 (100.0)	5 (100.0)	4 (66.7)	
Vascular Invasion					
No	7 (38.9)	6 (20.7)	12 (54.5)	1 (4.3)	**0.001**
Yes	11 (61.1)	23 (79.3)	10 (45.5)	22 (95.7)	
Perineural Invasion					
No	11 (61.1)	13 (44.8)	15 (68.2)	12 (52.2)	0.376
Yes	7 (38.9)	16 (55.2)	7 (31.8)	11 (47.8)	

CRM: Circumferential resection margin

Supplementary Table S3. Primer sets of 21 exons of human RecQL4 gene for PCR-SSCP analysis (Exon 5 was divided into three fragments: E5.1-E5.3)

SSCP Primers Design			
primer name	primer sequence(F)	primer sequence(R)	Product size(bp)
E1	GGAGATTCGCTGGACGAT	CTGTAAAGGGAACGCGTCAG	200
E2-E3	CTGACGCGTTCCCTTTACA	AAACAGGGAAGTGGGAGGAG	286
E4	ACAGCCTTTTCTGGCCTGT	GAAGCAGCTGTGGACCTAGC	228
E5.1	CCTGAGTTCCTCCTGCTGTT	CGACTCACCAGGGATCAGAA	359
E5.2	GCCTGATCTAGGCTCAGAGG	TGGAGGGTCTTCCTCAACTG	271
E5.3	CAGTTGAGGAAGACCCTCCA	AAAGGGAATGCCTGTCCTG	290
E6	CCCAGTGACCCTCCTATGTG	CTCCAGGGCAGATGTCTCAC	179
E7	GCTCCCATTCTACCCTCTCC	TGACTTGAGTCACCCCAACC	222
E8	GGGTGACTCAAGTCATGGTGA	GTGGAGATGCCTGGATGG	220
E9	CAGAACCCTGCTGCTGACTC	AAGTGCTGGTTCTTGGCTGT	220
E10	GCTGTCGCTCCTGCATTT	CTGCCTCCCTCACCCCTA	142
E11	CCTCTGATCTTGCTGCCTTC	CCCAGTTCACATATGGCTCA	217
E12	GCAAGGTGAGCCATATGTGA	GGTCCCCAGAGCACACAC	290
E13	GCCAACCGCTCCTCATC	ACACCAGCTCTGTCCATGC	185
E14	CACTGACCATCTGCCTGTCT	GGTGGGGTGGACCACTG	350
E15	CACCCCACCCTCATGAAA	GCTTACCCCAGGTTCCTCAC	342
E16	GGGTAAGCCACAGGGGTGT	CTCCAACCTCGTCTCCAACT	230
E17	GGCCACATGTCCCTTTTTC	GGAAAGCATGTCAGATGCAG	262
E18	CTGCATCTGACATGCTTTCC	CTACGCTGTGGGGAGGAG	287
E19	ACAGGCTCCTCCCCACAG	CCTGGCCTTACTGCACTCAC	195
E20	GAAGCCTGATGTGCCTGTC	CAAGACACAGCCGTGAGC	248
E21	GTGTCTTGGCTCCACCGTAG	CTGCCCTAGCCTCTGACAAC	200

Supplementary Table S4. PCR primer sets of drug-resistance related genes used for real-time RT-PCR analysis

Gene name		Sequence	Length (bp)
MRP1	F	AAGGGATCGCCGTGTTTGG	428
	R	CGAAGGCTCGAATGACGCTGAC	
MRP2	F	CCTGGTTCCTGTCCCTATTCT	472
	R	GGCATCTTGGCTTTGACTCTG	
MRP3	F	CGCCACAGTCCTTCTTTGACACCAC	443
	R	CCACGAACTCCACTCCGATGCTC	
MRP4	F	TTGGGATAAGGCATCAGAGACC	463
	R	AGTGTCTGCTAACTTCCGCATCTAC	
BCRP	F	GGCCTATAATAACCCTGCAGACTTC	391
	R	GCCCAAAGTAAATGGCACCT	
MVP	F	TTTGATGTCACAGGGCAAGTTCGGC	425
	R	CACCAAATCCAGAACCTCCTCAAAC	
MDR1	F	GAGCCCATCCTGTTTGACTGC	411
	R	TGCCATGCTCCTTGACTCTGC	
β-actin	F	AGCGAGCATCCCCCAAAGTT	284
	R	GGGCACGAAGGCTCATCATT	

Contents of Supplementary Materials and methods

1. Construction of Tissue Microarray (TMA)
2. Chemicals
3. Real-time PCR
4. Dual-Luciferase assay for MVP
5. *In vitro* pull-down assay
6. Co-immunoprecipitation
7. Protein expression and purification
8. Chromatin immunoprecipitation analysis
9. Electrophoretic mobility shift assays (EMSAs)
10. PCR-SSCP protocol

Construction of Tissue Microarray (TMA): TMAs were constructed. In short, area-specialized histopathologists identified and marked formalin-fixed paraffin-embedded tissue blocks containing tumor tissue on haematoxylin and eosin stained slides. The marked areas in these donor paraffin blocks were used to construct the tissue microarray. Triplicate tissue cores with a diameter of 0.6 mm were taken from the marked areas and arrayed into a recipient paraffin block using a tissue puncher/arrayer (Beecher Instruments, Silver Spring, MD, USA). Five micron sections of the tissue array block were cut and placed on microscope slides (Fisher scientific, Pittsburgh, PA) for immunohistochemical staining.

Chemicals

Cisplatin and p-Akt inhibitor MK-2206 were purchased from Sigma (St. Louis, MO, USA) and Selleck (#cat s1078), respectively, and dissolved in DMSO and stored at -20°C. Lipofectamine and Trizol reagent were from Invitrogen. Wizard Genomic DNA Purification Kit and moloney murine leukemia virus (MMLV) reverse transcriptase were from Promega (USA).

Real-time RT-PCR

The mRNA level for RecQL4 and a list of drug resistance-related genes was quantified by Real-time RT-PCR. The primer sets for drug resistance-related genes were listed in Supplementary Table S4. All reactions were done in triplicate and three independent experiments were performed. RT-PCR amplification results were calculated by CFX Manager. The real time PCR primers for *RecQL4* are: P1: 5'-TCACAGTGAGGTCCCAGATT-3' and P2: 5'-CTGACTTCTTGGAAGGCTG A-3'. *β-actin* was used as the internal control for normalization of RecQL4 mRNA.

Dual-Luciferase assay for MVP

MVP gene promoter region (from-679 to +23) containing Y-box consensus sequence used for luciferase reporter assay was amplified by PCR using the following primer pair: forward: 5'-ggggtaccCGTACCTGCTGGAGCCTGG-3', reverse: 5'-cccaagcttCCAGGCTCCAGCAGGTACG-3'. The PCR fragment was then cloned into the KpnI/HindIII sites of pGL3-Basic vector, and verified by sequencing. The pGL3-MDR1pro plasmid was transiently transfected into YB1-silenced MGC803/Tet-on/Flag-RecQL4 cells with YB1 reconstitution or/and Dox-induced expression of RecQL4. Luciferase activity was measured following the dual-luciferase assay protocol (Promega).

***In vitro* pull-down assay**

For RecQL4 pull-down YB1 assay, purified His-RecQL4-Flag fusion protein were bound to Flag M2 beads in buffer A (50 mM Na_2HPO_4, 150 mM NaCl, 10 mM EDTA, 0.2-0.5% NP-40, 2 mM DTT, pH7.5) and then incubated with His-YB1 fusion protein at 4°C for 2 h. The resins were washed, and the bound protein was detected by Western blotting.

Interactions among RecQL4, YB1 and Akt were then tested by pull-down assay. In brief, the bait protein was expressed as a (GST-Akt) fusion protein in *E. coli,* purifed and immobilized on Glutathione resin. Purified His-RecQL4-Flag or/and His-YB1 was added to the immobilized GST-Akt in buffer A. After gentle rotation at 4°C for 2 h, the bound proteins were examined by Western blotting.

To test whether or not RecQL4 promotes the association between Akt and YB1, a pull-down assay was further performed by immobilizing 3 μg of GST-Akt on Glutathione resin, followed by addition of 1 μg of His-YB1 combined with different amounts of His-RecQL4-Flag protein including 0, 0.2 μg (+) and 1 μg (++),

respectively. Level of YB1 in the bound protein was then quantified by the band intensity detected by Western blotting.

Co-immunoprecipitation

293T cells transfected with Flag-RecQL4 or Flag-GFP were collected in lysis buffer (50 mM Tris-HCl pH 7.5, 150 mM NaCl, 1% NP-40, 5 mM EDTA, 5 mM EGTA, 20 mM NaF, 0.1 mM PMSF, 0.5 mM benzamidine, 1 mg/ml leupeptin, 1 mg/ml aprotinin, 2 mM microcystin and 0.1 mM $NaVO_3$), and then incubated with anti-Flag-M2 beads (Sigma) at 4°C for 2 h. U2OS cells were harvested in lysis buffer and then incubated with Dynabeads Protein A that are coated with IgG or anti-YB1 antibody. After washing with lysis buffer, the binding complex was heated at 80°C for 10 min in 1×Laemmli buffer. The RecQL4 complex was visualized by Western Blotting.

Protein expression and purification

His-YB1 fusion proteins were constructed by cloning full-length human YB-1 into a pET-28a vector (Novagen). GST-Akt fusion proteins were constructed by cloning full-length human Akt into a pGEX-6p-1 vector (GE Healthcare). The plasmids were expressed in BL21 Escherichia coli and induced to express the fusion proteins with 0.5 mM isopropyl-b-D-thiogalactoside for 3 h at 37°C. The fusion proteins were purified by following His or GST tag purification method. Flag-RecQL4 fusion protein was constructed by cloning full-length human RecQL4 into pET-16b vector (Novagen). Fusion proteins were expressed in Rosetta (DE3) pLysS cells. Cells were grown at 37°C to a cell density OD600 0.4～0.5, followed by overnight induction at 16°C with 0.1 mM isopropyl-β-d-thio-galactoside. Cells were harvested and lysed in lysis buffer, followed by sonication. The supernatant was applied to Ni-NTA column, washed and eluted. The eluate was dialyzed and incubated with anti-FLAG M2 beads (Sigma). The M2-bound proteins were washed, eluted and dialyzed.

Chromatin immunoprecipitation analysis

Chromatin immunoprecipitation (ChIP) assays were carried out as previously

described (Zhang Y., et al, Cancer Res., 2009). 1×107 MGC-803 cells were fixed with 1% molecular grade formaldehyde (Sigma) and sonicated with Bioruptor® Plus device. YB1 antibody was used for immunoprecipitation and detected with quantitative PCR (BioRad CFX-96 Real-Time PCR System). Data were analyzed by delta Ct method. Primers for human MDR1 gene were 5-ACCTGTTTCGCAGTTTCTCG -3 (forward) and 5- GAAGAGCCGCTACTCG AATG -3 (reverse). Primers used for negative control were 5-AGGTGGAGAAACACCACCAC-3 (forward) and 5-CGGTTTGCCCAAG AAAAATA-3 (reverse).

Electrophoretic mobility shift assays (EMSAs)

The 5' Digoxin-labeled oligonucleotide contained the WT (5'-GGTGAGGCTGATTGGCTGGGCAGGA-3') or mutated Y box (5'-GGTGAGGCTGATCAACTGGGCAGGA-3') (underlined WT and mutated Y-box sequences were annealed with appropriate complementary stands to generate the duplex oligonucleotides)(Chattopadhyay R., Mol. Cell Biol., 2008). Each oligonucleotide (20 ng) was then incubated with 100 ng of YB-1 or YB-1 smaller segment (130 to 205 aa) and RecQl4 (100 ng) for 20 min at 25°C in a buffer containing 40 mM HEPES-KOH (pH 7.5), 50 mM KCl, 1 mM MgCl2, 0.5 mM EDTA, 0.5 mM dithiothreitol, 10% glycerol, and 1 μg of poly(dI-dC) (Sigma). After electrophoresis in nondenaturing 6% polyacrylamide gels in Tris-borate buffer at 4°C, the gels were transferred and crosslinked for 120 mJ/cm2 by Bio-Link Crosslinker BLX-E254. Binding reactions were performed using a LightShift Chemoluminescent EMSA Kit according to the manufacturer's instructions (Thermofisher).

PCR-SSCP protocol

2 μl PCR product and 10 μl loading buffer (10% sucrose with a little bromophenol blue) is denatured at 95°C for 10 minutes and immediately kept on ice for 5 minutes, then the samples are loaded on a nondenaturing 8% acrylamide: bis-acrylamide (49:l) gel and immediately electrophoresis is performed in 1 X TBE buffer at 200 V for 1hr

at 4℃. After the electrophoresis, the gel is fixed in 10% methanol and 0.5% acetic acid for 10min on a shaker, then put the gel into 0.1% silver nitrate solution staining for 10min in dark on a shaker. The gel is rinsed briefly for 10 seconds in distilled water and the freshly prepared and chilled 1.5% sodium hydroxide solution (1.5% NaoH + 0.15% formaldehyde) is transferred to the tray. The gel is kept immersed until bands get developed sharply. Then gel is labeled and scanned for computer image analysis and documentation.